

DYNAMIC VOLTAGE STABILITY ANALYSIS

USING DECISION TREES

SAMSON NJUGUNA NJOROGE

MASTER OF SCIENCE

(Electrical Engineering)

JOMO KENYATTA UNIVERSITY OF

AGRICULTURE AND TECHNOLOGY

2016

Dynamic Voltage Stability Analysis Using Decision Trees

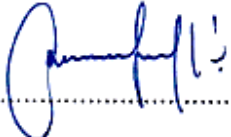
Samson Njuguna Njoroge

**A thesis submitted in partial fulfillment of the requirements for
the award of the degree of Master of Science in Electrical
Engineering in the Jomo Kenyatta University of Agriculture and
Technology.**

2016

DECLARATION

This thesis is my original work and has not been presented for a degree in any other university.

Signature: .....

Samson Njuguna Njoroge

Date: 28-04-2016.....

This thesis has been submitted for examination with our approval as university supervisors:

Signature: .....

Dr. Christopher Maina Muriithi

Technical University of Kenya

Date: 28/04/2016.....

Signature: .....

Prof. Livingstone M. H. Ngoo

Multimedia University of Kenya

Date: 28/4/16.....

ACKNOWLEDGEMENT

Many people have contributed to this piece of work;

To God for the gift of life and knowledge, grace and mercy through all stages of my learning culminating in this thesis. For His grace, mercy and provision, I'll be eternally indebted and thankful. May His name always be praised.

My supervisors, Dr. Christopher M. Maina and Prof. Livingstone M. H. Ngoo for their indefatigable inspiration, guidance, instruction and insight in the full course of the research.

My family; Frida, Wanjiku and the rest for their prayers and support in many ways throughout my journey, especially in the course of this research and for being the inspiration for me to complete when things got tough in the course of my research,

All my classmates, especially in the Power Systems Option for their support and encouragement,

All the staff of Electrical and Electronic Engineering Department, JKUAT who imparted helpful knowledge and assisted in developing and carrying out this research,

And lastly, all scientists, past and present, who inspired me by seeking to better understand God's creation, and hence improve our lives by it.

TABLE OF CONTENTS

DECLARATION	i
ACKNOWLEDGEMENT	ii
TABLE OF CONTENTS.....	iii
LIST OF FIGURES	vii
LIST OF TABLES	xi
LIST OF APPENDICES.....	xii
ABBREVIATIONS	xiii
ABSTRACT	xv
CHAPTER ONE	1
INTRODUCTION	1
1.1 Background	1
1.2 Problem Statement.....	2
1.3 Justification	3
1.4 Objectives	3
1.4.1 Main Objective	3
1.4.2 Specific Objectives	3
1.5 Scope.....	3
1.6 Thesis Organization.....	4
1.7 Journal Papers Published from this Thesis	4

1.8 Conclusion	5
CHAPTER TWO	6
LITERATURE REVIEW	6
2.1 Introduction.....	6
2.2 Power System Stability	6
2.3 Voltage Stability	6
2.4 Voltage Stability Indices.....	9
2.4.1 PV and QV Curves.....	9
2.4.2 VCPI Index.....	10
2.4.3 VV0 Index.....	11
2.4.4 FVSI Index	12
2.4.5 <i>Lmn</i> Index	12
2.4.6 LQP Index.....	13
2.5 Power Flow Analysis.....	14
2.6 Artificial Intelligence.....	14
2.6.1 Fuzzy Logic	15
2.6.2 Artificial Neural Networks	15
2.6.3 Decision Trees	16
2.6.3.1 ID3 Decision Trees.....	21
2.6.3.2 C4.5 Decision Trees	21

2.6.3.3 Classification and Regression Trees (CART).....	22
2.7 Previous Works	23
2.8 Conclusion	27
CHAPTER THREE	29
METHODOLOGY	29
3.1 Introduction.....	29
3.2 Verification of VCPI Parameters - IEEE 9 – Bus System.....	30
3.3 Application of VCPI with ANN - IEEE 30 – Bus System	31
3.4 VCPI with ANN Based Analysis - Kenya Power System.....	35
3.5 Developing of CART Algorithm – IEEE 30 – Bus System	39
3.6 CART Based Analysis - Kenya Power System.....	42
3.7 Conclusion	43
CHAPTER FOUR.....	44
RESULTS AND ANALYSIS.....	44
4.1 Introduction.....	44
4.2 Verification of VCPI Parameters - IEEE 9 – Bus System.....	44
4.3 Application of VCPI with ANN - IEEE 30 – Bus System	45
4.4 VCPI with ANN Based Analysis - Kenya Power System.....	47
4.5 Developing of CART Algorithm using the IEEE 30 – Bus System	52
4.6 CART Based Analysis - Kenya Power System.....	54

4.7 Conclusion	59
CHAPTER FIVE	60
CONCLUSIONS AND RECOMMENDATIONS.....	60
REFERENCES	63
APPENDIX	66

LIST OF FIGURES

Figure 2.1: PV Curve.....	9
Figure 2.2: QV Curve.....	10
Figure 2.3: Artificial Neuron Model.....	16
Figure 2.4: Decision Tree Example.....	17
Figure 2.5: Comparison of DT Impurity Measures.....	20
Figure 3.1: IEEE 9 – Bus System.....	30
Figure 3.2: VCPI Calculation Algorithm for IEEE 9 - Bus (Bus 5)	31
Figure 3.3: IEEE 30 – Bus System.....	32
Figure 3.4(a): VCPI – Line Contingency Simulation.....	34
Figure 3.4(b) : VCPI - Bus Loading Variation.....	35
Figure 3.5: Kenya Power System.....	36
Figure 3.6(a): VCPI Application - Kenya Power System – Load Flow Calculation.....	37
Figure 3.6(b): VCPI Application - Kenya Power System – Load Variation.....	38
Figure 3.7: VCPI at 95% Weak Bus Voltage Drop – Kenya Power System.....	39
Figure 3.8: CART Construction Algorithm – IEEE 30 – Bus System.....	41

Figure 3.9(a): CART Construction Algorithm – Kenya Power System – Load Flow Calculation	42
Figure 3.9(b): CART Construction Algorithm – Kenya Power System – Load Variation	43
Figure 4.1: VCPI and Voltage at bus 5 for bus 5 loading – IEEE 9 - Bus System.....	44
Figure 4.2: VCPI and Voltage at bus 10 for bus 10 loading – Kenya Power System.....	47
Figure 4.3: VCPI and Voltage at bus 30 for bus 10 loading – Kenya Power System.....	48
Figure 4.4: VCPI and Voltage at bus 30 for bus 30 loading – Kenya Power System.....	48
Figure 4.5: VCPI and Voltage at bus 10 for bus 30 loading – Kenya Power System.....	49
Figure 4.6: CART Tree (3000 Minimum Observations) Bus 26 – IEEE 30 Bus System.....	52
Figure 4.7: CART Tree (4000 Minimum Observations) Bus 26 – IEEE 30 Bus System....	54
Figure 4.8: CART Tree (Pruned 2 levels) Bus 26 – IEEE 30 Bus System.....	54

Figure 4.9: CART Tree (3500 Minimum Observations) Bus 10 – Kenya Power System.....	55
Figure 4.10: CART Tree (Level 2 Pruned) Bus 10 – Kenya Power System.....	56
Figure 4.11: CART Tree (3500 Minimum Observations) Bus 30 – Kenya Power System.....	57
Figure 4.12: CART Tree (Level 1 Pruned) Bus 30 – Kenya Power System.....	58
Figure A1: IEEE 9 – Bus System.....	66
Figure A2: IEEE 30 – Bus System.....	67
Figure A3: Kenya Power System.....	70
Figure A5.1: CART Tree (3500 Minimum Observations) Bus 2 – Kenya Power System.....	74
Figure A5.2: CART Tree (3500 Minimum Observations) Bus 3 – Kenya Power System.....	74
Figure A5.3: CART Tree (3500 Minimum Observations) Bus 4 – Kenya Power System.....	75
Figure A5.4: CART Tree (3500 Minimum Observations) Bus 8 – Kenya Power System.....	75
Figure A5.5: CART Tree (3500 Minimum Observations) Bus 13 – Kenya Power System.....	76

Figure A5.6: CART Tree (3500 Minimum Observations) Bus 15 – Kenya Power System.....	76
Figure A5.7: CART Tree (3500 Minimum Observations) Bus 26 – Kenya Power System.....	77
Figure A5.8: CART Tree (3500 Minimum Observations) Bus 31 – Kenya Power System.....	77

LIST OF TABLES

Table 4.1: Comparison of VCPI using Load Flow and ANN (Bus 26 – IEEE 30 - Bus System)	46
Table 4.2: Comparison of VCPI using Load Flow and ANN (Bus 10 – Kenya Power System)	50
Table 4.3: Comparison of VCPI using Load Flow and ANN (Bus 30 – Kenya Power System)	51
Table A.1: IEEE 9 – Bus System Bus Data.....	66
Table A.2: IEEE 9 – Bus System Line Data.....	67
Table A.3: IEEE 30 – Bus System Bus Data.....	68
Table A.4: IEEE 30 – Bus System Line Data.....	69
Table A.5: Kenya Power System Bus Data.....	71
Table A.6: Kenya Power System Line Data.....	72
Table A.7: Comparison of VCPI Values Using Load Flow Calculations and ANNs for IEEE 14 – Bus System [25]	73

LIST OF APPENDICES

Appendix A1: IEEE 9 - Bus System.....	66
Appendix A2: IEEE 30 - Bus System.....	67
Appendix A3: Kenya Power System (37-Bus Model).....	70
Appendix A4: ANN vs Load Flow Calculation for VCPI Calculation.....	73
Appendix A5: Selected CART Decision Trees For Kenya Power System Load Buses.....	74

ABBREVIATIONS

AC	Alternating Current
ANN	Artificial Neural Network
ANSI	American National Standard Institute
AVR	Automatic Voltage Regulator
CART	Classification and Decision Trees
CPANN	Counter Propagating Artificial Neural Networks
DT	Decision Trees
FACTS	Flexible AC Transmission Systems
GB	Giga – Bytes
GHz	Giga – Hertz
IEEE	Institute of Electrical and Electronic Engineers
KB	Knowledge Base
MIMO	Multiple Input Multiple Output
MVA	Mega – Volt – Ampere
MVAR	Mega – Volt – Ampere – Reactive
MW	Mega-Watts
OP	Operating Points

PTSI	Power Transfer Stability Index
PU	Per Unit
RAM	Random Access Memory
RBFNN	Radial Basis Function Neural Network
SCADA	Supervisory Control And Data Acquisition
STATCOM	Static Compensator
SVC	Static VAR Compensator
VAR	Volt Ampere Reactive
VCPI	Voltage Collapse Proximity Indicator

ABSTRACT

All over the world, power systems are being operated in more stressed conditions as modernisation and globalization increase demand for electricity. In Kenya, the government has in the last few years been on a drive to connect more consumers to the national grid in line with its Vision 2030. The national electricity distribution utility, Kenya Power Company, has been on a drive to connect 300,000 new customers each year to the grid since 2009 while the Rural Electrification Authority was established in 2007 and is mandated with connecting rural customers. The increase in the consumer load has however not been matched by increase in the generation.

Consequently, the system is operated closer to its stability limit and is thus more prone to instability in case of contingencies as was witnessed during the April - June 2012 long rains when the system experienced nationwide blackouts. It further puts pressure on system controllers to operate the system within the lower security margins and defensively operate the system during conditions of peak loads.

This research thesis aimed at evaluating the dynamic voltage security of the Kenya Power System using decision trees. These would establish the real time voltage security status of the system and the likely final voltage stability status if the system is allowed to continue operating with the given loading – contingency configuration. This would allow system operators to quickly establish the voltage stability status of the system. At the same time, it will help in indicating how close the voltage insecure buses are to voltage collapse by using an Artificial Neural Network (ANN) based proximity-to-collapse index instead of the conventional Continuation Power Flow (CPF) which takes a lot of computing effort. Dynamic Voltage stability analysis of any system is studied by considering load changes within the system and how voltage magnitudes at the load buses within the system are affected by the load changes. The analysis can be further complicated by considering probable contingencies within the system that are caused by line outages. The dynamic nature of the load can be considered by using dynamic load models and evaluating the changes, with time, of the bus voltages. However, the model-driven voltages take

time to compute which may not give the system operator time to act since voltage collapse occurs within a very short period.

This research considered 100 random load variations without regard to power factor for each probable single – line outage. This gave many snapshots of the dynamic load from which the dynamic tendency of the system was then evaluated by constructing a decision tree for each load bus within the system. The algorithm was first validated on the IEEE test systems (9 - Bus and 30 - Bus) before being applied to the Kenya Power System.

The Decision Trees show the relationship between a particular bus's voltage magnitude and the contingency and power demand at other buses. The results demonstrated relationships between bus power demands and voltages at other buses that would otherwise not be visible by simply evaluating load flow studies from static snapshots of the Kenyan system. The resulting decision trees for the buses within the Kenya Power System show the most influential variable at each bus and give a binary split for each variable, and the expected voltage magnitude at that bus.

CHAPTER ONE

INTRODUCTION

1.1 Background

A power system is an interconnection of generators, transmission lines and electrical loads which form a large network. Various other devices such as transformers are introduced into the system to make it feasible to increase the power transmission capacity from the generators to the loads using the transmission lines. The nature of the transmission lines and the loads distributed over large distances makes the buses' voltage magnitudes within the power system to fall below optimum operating values. Faults or contingencies as well as load changes also vary the voltage and generator angles within the system.

Voltage stability analysis interrogates the ability of the power system to maintain the voltage magnitude at all buses within a small operating margin. The mathematical nature of the analysis means it takes time to carry out a stability analysis, whether static or dynamic. The advent of modern technologies such as artificial intelligence techniques has reduced the time it takes to carry out voltage stability analyses leading to the development of design tools that can evaluate voltage stability even on an online basis.

Traditionally, dynamic voltage stability analysis is studied with a time aspect which shows how the voltage at a bus changes as load variations occur with time. This analysis is difficult to evaluate on a real time basis for all buses as the techniques used take a lot of computational effort. Additionally, the existing methods such as singular value decomposition while able to evaluate the dynamic voltage stability of the entire system can only work with a single system layout at a time and require to be recalculated for each change in the system configuration. Also, they can only give the mechanism through which voltage collapse could occur in a system but not how close the system is to collapse. Other tools such as PV curves and QV curves can only tell the margin of loading allowable at a bus before its voltage dips below

allowable levels but require to be computed for each bus for every single change in system loading configuration.

In order to address the shortcomings of these methods, an alternative is to take multiple static snapshots of the system as it varies with time. Doing so means that the analysis is limited to linear equations which can be solved using the conventional load flow calculation. By having sufficient static snapshots of the system from the initial base case conditions, it is then possible to perform a dynamic analysis of the whole system. By using predictive artificial intelligence techniques such as Artificial Neural Networks (ANNs) and decision trees, it then becomes possible to create a predictive model of the system, which can be used dynamically by predicting voltage magnitudes at load buses as the loads vary with time making it possible to predict the safety margin before voltage collapse occurs.

This research thesis aimed at exploiting the potential of Decision Trees to carry out dynamic voltage stability analysis on the Kenya Power System. The decisions trees are developed from multiple loading and single – line outage conditions which simulate dynamic operating conditions. The resulting decision trees can then be used to develop an online dynamic voltage stability monitoring tool.

1.2 Problem Statement

Operating a system close to its loading limit reduces the safety margin of operation and makes the system more unstable in case of any contingency occurring. However, economic reasons limit the expansion of transmission and generation capacity hence the system is gradually operated closer to its loading limit as more customers are connected to the grid. As a result of the increased loading at the buses, the voltage magnitudes at heavily loaded buses will drop. This drop further reduces the capacity of transmission lines to transmit power which further compounds the problem, especially if there is a contingency affecting a transmission line within the system. While the system operator may have real time readings of voltage magnitudes at each bus, this may not be the case in quickly determining how much more load can be added to a particular bus without its voltage dropping below viable operation levels. Further, this may not also show which buses will be adversely affected by a line

contingency occurring within the system, or how the loading at one bus affects the voltage magnitude at another bus.

1.3 Justification

Conventional dynamic voltage stability analysis methods such as modal analysis and continuation power flow require a lot of computational effort and take considerably more time to compute. In addition, some methods require to be computed repeatedly for each change in the systems loading configuration. However, the power system takes a very short time to slip dynamically from a stable operating condition to an unstable condition. By using artificial intelligence technologies like artificial neural networks and decision trees, the time taken to predict the voltage stability of a particular bus can be reduced considerably. This gives the system operator more time to take remedial measures to avoid voltage collapse and enables defensive operation of the system.

1.4 Objectives

1.4.1 Main Objective

The main objective of this thesis was to perform dynamic voltage stability analysis of the Kenya power system using decision trees and to suggest possible mitigation measures of voltage instability.

1.4.2 Specific Objectives

- i. To carry out load flow studies on the Kenyan system and identify weak buses
- ii. To construct decision trees for analyzing dynamic voltage stability for the Kenya Power System
- iii. To suggest possible mitigation measures for dynamic voltage instability

1.5 Scope

The scope of this research was limited to the Kenya Power System, (1996) model. The IEEE 9 – Bus System and the IEEE 30 – Bus system were also used in validating the various algorithms. An MVA base of 100MVA was adopted for all the systems. The base case values for the IEEE 9 – Bus System and the IEEE 30 – Bus

system are given in appendix A1 and A2 respectively. The base case values for the Kenya Power System are given in appendix A3. Dynamic voltage stability analysis was achieved by use of multiple static power flow analyses. The research was also limited to the use of the Voltage Collapse Proximity Indicator (VCPI) index and the Classification And Regression Tree (CART) decision trees.

1.6 Thesis Organization

Chapter 1

This chapter presents an overview of the various sections and the work they cover within this thesis. The breakdown of the rest of the thesis is given in the following sections:

Chapter 2

This chapter presents a literature review on Power Systems Stability, Voltage Stability, Load Flow Studies and Artificial Intelligence Techniques. It also gives a review of recent works related to dynamic voltage stability and decision trees

Chapter 3

This chapter gives an overview of the methodology followed in performing this research.

Chapter 4

This chapter presents the results obtained from the analysis and accompanying discussion and analyses of the results

Chapter 5

This chapter presents a conclusion of the work and gives recommendations for future research

1.7 Journal Papers Published from this Thesis

From this research, the following journal papers have been published;

1. *Dynamic Voltage Stability Analysis of the Kenya Power System Using VCPI Stability Index and Artificial Neural Networks*, S. N. Njoroge, C. M. Muriithi and L. M. H. Ngoo, European International Journal of Science and Technology, Vol. 3(7) September, 2014, pp. 23-30.

2. *Dynamic Voltage Stability Analysis of the Kenya Power System Using Decision Trees*, S. N. Njoroge, C. M. Muriithi and L. M. H. Ngoo, International Organisation of Scientific Research, Vol. 04 Issue 12 December, 2014, pp. 20-24 .

1.8 Conclusion

In this chapter, a brief introduction of voltage stability is given. In addition, the problem statement, justification, objectives and scope of this thesis is outlined. Additionally, an outline of the thesis is given as well as a list of publications derived from the content of the research.

CHAPTER TWO

LITERATURE REVIEW

2.1 Introduction

In this chapter, a review of power flow studies, voltage stability and various techniques used in the evaluation of voltage stability analysis are given. Several artificial intelligence techniques are also reviewed. This background forms a basis that will be referred to in the rest of the thesis.

2.2 Power System Stability

Power system stability is the ability of a power system to remain in a state of operating equilibrium under normal operating conditions and to regain an acceptable state of equilibrium after being subjected to a disturbance [1]. The main parts of a power system are the generators, the transmission lines and the loads. Generators generate the electrical energy mostly at the sources which are natural resources like steam, water in dams or wind. Transmission lines transfer the energy from the generation locations to the loads which are the energy consumption centers and are located at human settlement locations and industrial installations. The loads are connected to the system through buses which are electrical nodes. Power system stability can be viewed from either the generator and its rotor stability and frequency stability or from the load buses' voltage stability. This thesis focuses on the voltage stability.

2.3 Voltage Stability

Voltage Stability is the ability of a power system to maintain steady acceptable voltages at all buses in the system under normal operating conditions and after being subjected to a disturbance [1]. Voltage Stability may also be described as the ability of a system to maintain voltage magnitudes so that when load admittance is increased, load power will increase, and so that both power and voltage are controllable [2]. A power system at a given operating state and subject to a given disturbance is *voltage stable* if voltages near loads approach pre-disturbance equilibrium values. The disturbed state is within the region of attraction of the stable

post-disturbance equilibrium [3]. Devices connected at the load buses are designed to operate at a particular rated voltage. An increase beyond this voltage is likely to damage the devices and incur losses to the customer and the utility. Conversely, a drop beyond the rated voltage will affect the devices' normal operation. Static devices will tend not to function properly as the power transmitted to them will drop since power is a product of the voltage and current. Dynamic loads, especially inductive motor loads, will tend to draw more current above the rated current so as to compensate for the reduced voltage and still meet the load torque demand. This has the effect of lowering the bus voltage even further, leading to a voltage collapse at that particular bus. Since it is also not practical to operate the system at a static constant voltage, a small margin of voltage oscillation is normally provided. In general, the voltages of the buses within a power system are required to remain within a particular margin from the specified voltage. Most systems have this margin as 4% or 5% of the nominal bus voltage in line with ANSI standard C84.1. Voltage Stability can further be classified as either Static Voltage Stability or Dynamic Voltage Stability depending on the time frame of reference of the stability analysis. Further, voltage stability can be studied in terms of the proximity to voltage collapse or the mechanism of voltage collapse [4].

Proximity to Voltage Collapse is concerned with how close the system voltage is to collapse. This "distance to collapse" can be quantified in terms of loading levels, active power flow through a critical line or reactive power reserve within a system. More recently, voltage stability indices that combine many parameters into one index have been developed that indicate the distance to collapse in terms of an index.

Mechanism of Voltage Collapse is concerned with the how and why of voltage instability occurrence by looking at the contributing factors to voltage instability in a system. Time domain simulations are ideal for this method of voltage stability analysis but since the parameters affecting voltage stability are slow acting, static analyses taking snapshots of probable operating conditions can be used to validly point out the mechanism of voltage collapse in a system for different operating conditions [1].

Dynamic Voltage Stability Analysis deals with how the bus voltages change with changes in system operating parameters. It is useful in detailed studies of voltage collapse situations and also for coordination of protection devices and controls within a healthy power system by identifying the system elements that will contribute first to a voltage collapse situation and setting the protection devices to isolate these elements first. It is also useful in simulation of remedial measures to possible contingencies within a system to see if they can adequately protect the system from collapse.

Dynamic voltage stability analysis can be carried out by analysing the system as follows;

A power system can be represented as a system of first order differential equations which can be written in general as

$$\dot{\mathbf{x}} = f(\mathbf{x}, \mathbf{V}) \quad (2.1)$$

as well as the algebraic equations

$$\mathbf{I}(\mathbf{x}, \mathbf{V}) = \mathbf{Y}_N \mathbf{V} \quad (2.2)$$

When starting with a set of initial operating conditions $(\mathbf{x}_0, \mathbf{V}_0)$

Where

\mathbf{x} – state vector of the system

\mathbf{V} – bus voltage vector

\mathbf{I} – current injection vector

\mathbf{Y}_N – network node admittance matrix

The solution of equations (2.1) and (2.2) represents the dynamic state of the system and is usually studied for several minutes to see the changes occurring in the system during the period. The methods of solution for equations (2.1) and (2.2) can be numerical integration in the time domain. More recently, methods like singular value analysis have been used in dynamic voltage stability analysis [5,6].

2.4 Voltage Stability Indices

In considering the dynamic voltage stability of a system, the proximity to collapse is a critical factor to be evaluated. Voltage stability indices provide a means of evaluating various parameters in a system with a view of establishing how close the system is to voltage collapse and allowing for defensive measures to be taken to avert the collapse. Several indices exist that have been used in voltage stability analysis as discussed in the sections below;

2.4.1 PV and QV Curves

The loading margin provides the most accepted method of approximating proximity to voltage collapse. From a static stable operating point on a particular bus, the total increment in loading that can occur and following a particular loading pattern can be plotted using either a PV curve (Figure 2.1) or a QV curve (Figure 2.2)[7].

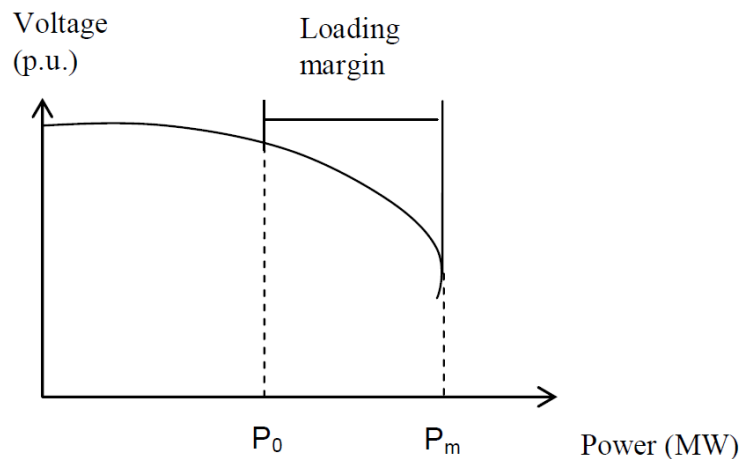


Figure 2.1: PV Curve

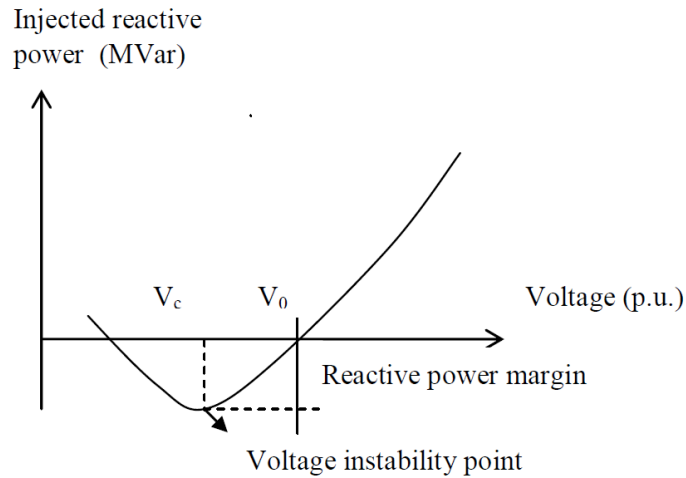


Figure 2.2: QV Curve

The increment of the loading which is done by simulation is stopped at the nose of the curve which is the voltage collapse point. Realistically, only during the simulation can a system arrive at the nose of the PV curve. A real system would have collapsed by the time it reaches this point. From the resulting curve, the loading margin or reserve is the distance from the current operating point on the curve to the maximum loading point on the curve and represents the distance to collapse in MW or MVAR. In Figure 2.1, P_0 is the load power at the current operating point, and P_m is the maximum active power that the load can consume from the system. In Figure 2.2, it is possible to know the maximum reactive power that can be drawn at a bus before reaching the minimum voltage limit. The curve can be produced by varying the reactive power demand at the load bus while maintaining the active power constant. The corresponding load voltage is determined through load flow recalculation. The reactive power margin is the MVAR distance from the operating point to the bottom of the Q-V curve.

2.4.2 VCPI Index

Another Voltage Stability Index is the VCPI (Voltage Collapse Proximity Indicator). It is developed using the voltage phasor information of the participating buses in the system and the system's admittance matrix [8], [26]. The technique draws from the basic power flow equations. From the solution of the power flow equations using the

Newton – Raphson method, a matrix of the output voltages for all the buses is obtained. This index is calculated at a bus for a particular loading condition [9] as;

$$L_j = \left| \frac{S_{j+}^*}{Y_{jj+} V_j^2} \right| \quad (2.3)$$

where

L_j – VCPI index ;

V_j – Voltage at bus j ;

S_j – Complex power at bus j

$$S_{j+} = S_j + S_{jcorr}$$

$$S_{jcorr} = \left\{ \sum_{\substack{i \in Loads \\ i \neq j}} \frac{Z_{ji}^* S_i}{Z_{jj}^* V_i} \right\} V_j$$

The VCPI is calculated for the load buses within the system. It has a value of 0 for stability and 1 for complete instability.

2.4.3 V/V_0 Index

A third index is the V/V_0 index. It is formulated for each bus by considering the variation of the bus voltage magnitude at no load to the nominal loading condition [26]. A load flow of the power system in question is performed with the base case system values with the loading of each bus at its nominal value and the voltage magnitude V at each bus recorded. After this, a second load flow is performed with all loads in the system set to 0. The resulting bus voltage magnitudes V_0 are then recorded. The ratio of V/V_0 at a bus is then its stability index. The index represents the variation of the voltage magnitude from the base case voltage magnitude. It has a value of 1 if the voltage magnitude during the loading condition is unchanged from the no-load condition. Alternatively, its value is greater than 1 if the on-load bus voltage is greater than the no load voltage and a value of less than 1 if the on-load

bus voltage is less than the no-load bus voltage. Since it gives a bus voltage as a ratio of the no-load voltage, it doesn't give the voltage in p.u. and hence depends on the value of the no load voltage. Although the V/V_0 is easy to compute for a single bus the main shortcoming it has is that it requires 2 load flows to compute, which would require a large computing capacity for multiple load changes.

2.4.4 FVSI Index

Another voltage stability index is the FVSI (Fast Voltage Stability Index) [27]. This index is calculated for a transmission line as

$$FVSI_{ij} = \frac{4Z^2Q_j}{V_i^2X} \quad (2.4)$$

Where

V_i is the sending end bus voltage

Q_j is the reactive power flow at the receiving end

Z is the line impedance

X is the line reactance

The main shortcoming is that the index was developed for a system having only one transmission line. For a heavily interconnected system, the FVSI has to be calculated at a bus for all lines connected to the bus. It helps in identifying the most critical line for a particular bus, and identifying critical lines within the whole system. It has a value of 0 for non – critical lines and 1 for the most critical lines.

2.4.5 L_{mn} Index

Yet another voltage stability index is the Line Stability Index L_{mn} index [28]. It is also based on a system with a single transmission line. The index is formulated as

$$L_{mn} = \frac{4XQ_j}{[V_i \sin(\theta - \delta)]^2} \quad (2.5)$$

Where

θ is the line impedance angle

δ is the angle between the sending end voltage and the receiving end voltage.

X is the line reactance

Q_j is the reactive power flow at the receiving end

Lines that exhibit values of L_{mn} close to 0 are stable while those with L_{mn} values approaching 1 are close to their instability points. Like the FVSI index, the L_{mn} index has to be calculated for all lines connected to a load bus. It's main disadvantage for this research was that it required to be calculated multiple times for a single bus.

2.4.6 LQP Index

Still another voltage stability index is the LQP line index [29]. The index takes into consideration the real and reactive power flow across a transmission line and is defined as

$$LQP = 4 \left(\frac{X}{V_i^2} \right) \left(\frac{X}{V_i^2} P_i^2 + Q_j \right) \quad (2.6)$$

Where

X is the line reactance

V_i is the voltage at the sending end

P_i is the active power flow at the sending end

Q_j is the reactive power flow at the receiving end bus

Voltage secure lines have a LQP value of less than 1. Like the other line based indices, the LQP index has to be calculated for all lines connected to a bus. It still has the shortcoming of being a line based index hence requiring multiple calculations for a single bus.

2.5 Power Flow Analysis

This analysis is also called Load Flow Analysis. It involves the calculation of load/power flows and voltages of a transmission network for specified terminal or bus conditions. Such calculations are required for the analysis of steady state and dynamic performance of power systems [1]. The system is assumed to be balanced allowing for a single phase representation and the generator, transmission lines and loads modeled to form network equations whose solution gives the power flow and voltages at all the buses within the system. The network equations for the i^{th} bus in the system are given by

$$P_i = |V_i| \sum_{k=1}^n |V_k| |Y_{ik}| \cos(\theta_{ik} + \delta_k - \delta_i) \quad ; i = 1, 2, \dots, n \quad (2.7)$$

$$Q_i = -|V_i| \sum_{k=1}^n |V_k| |Y_{ik}| \sin(\theta_{ik} + \delta_k - \delta_i) \quad ; i = 1, 2, \dots, n \quad (2.8)$$

Where n is the number of buses in the system [1].

The solution to these network equations is found using non-linear mathematical equation solution methods like the Gauss Seidel and Newton Raphson. The Newton Raphson method is preferred due to its quadratic convergence as compared to the linear convergence of the Gauss Seidel method. The Newton Raphson method was adopted in this research. Using this method, the Jacobian matrix is used to evaluate small changes in θ and V for small changes in P and Q .

$$\text{Jacobian} = \begin{bmatrix} \frac{\partial P}{\partial \theta} & \frac{\partial P}{\partial V} \\ \frac{\partial Q}{\partial \theta} & \frac{\partial Q}{\partial V} \end{bmatrix} = \begin{bmatrix} J_1 & J_2 \\ J_3 & J_4 \end{bmatrix} \quad (2.9)$$

The J_1 and J_3 components of the Jacobian matrix were used in this research.

2.6 Artificial Intelligence

These techniques are artificial replications of the natural workings found throughout nature. The difficulty of computing equations with many variables such as the power system equations has necessitated the borrowing of solutions from nature by

formulating algorithms from natural occurrences into mathematical equations and using them to finding solutions to complex non-linear problems. Normal computation technologies that simply automate mathematical formulae have the main disadvantage of taking comparatively long time to produce results mainly because they are exact methods. They also do not utilize the vast experience and wide knowledge that a system operator for instance may have. In comparison, artificial intelligence methods boast learning capability and are much faster as they use a knowledge base or learn trends to produce results for future problems

2.6.1 Fuzzy Logic

Fuzzy logic is based on fuzzy set theory. It operates on a set of IF-THEN rules which govern what the inputs will map to in the output. Input variables are members of input sets and the membership is weighted in membership functions depending on how well they can be described by the variables of that particular set. Similarly, output variables are members of output sets. Based on a knowledge base and past experience, IF-THEN rules are made that map between the input variables and output variables. The selected output is also weighted since the output membership set is a mathematical function. The resulting rules and sets form a Fuzzy Controller that can be used generically for a given application. The mathematical calculations involved are inbuilt in the simulation software hence once the rules have been written, fuzzy logic is faster than normal computational methods which require the user to make manual calculations.

2.6.2 Artificial Neural Networks

These mimic the human brain and consist of an interconnection of artificial neurons. Neural Networks can be defined as a class of mathematical algorithms designed to solve a specific problem [10]. Basically they are parallel computational models comprised of densely interconnected adaptive processing units. An extremely important and human characteristic of ANN is their adaptive nature, where learning by experience replaces programming in solving problems. ANN learn the pattern on which they are trained.

The fundamental building block in an Artificial Neural Network is the mathematical model of a neuron as shown in Fig. 2.3.

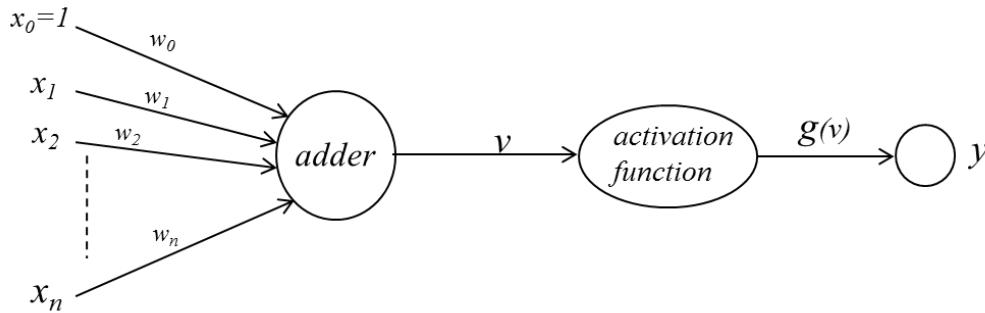


Figure 2.3: Artificial Neuron Model

The three basic components of the (artificial) neuron are the synapses that connect from the output of other neurons and have input weights, an adder that sums up the weighted inputs and an activation function that maps the output of the adder to the required output of the neuron as given in equations (2.11).

$$\text{Output } y = g(v) = g(x_0w_0 + x_1w_1 + \dots + x_nw_n) \quad (2.10)$$

ANNs can be trained in a supervised manner where input-output data sets are used to modify the weights and activation functions or in an unsupervised manner where only input sets are used to modify the weights of the input synapses.

2.6.3 Decision Trees

Decision Trees (DT) are not a new method though their uptake has been slow. They are based on the classical decision tree which involves splitting. Decision tree learning is a method commonly used in data mining. The goal is to create a model that predicts the value of a target variable based on several input variables. The variables are successively split into a dichotomy (binary) at each step according to a given criteria relating that variable to the selected output variables at the node. The variable with the greatest effect on the output variable is split first while the one with least observable effect is split last.

If we considered an example in medicine where the goal is to predict the obesity status of a child based on their bio – data, we may use 3 variables namely;

$$x_1 - \text{Weight} : x_2 - \text{Age} : x_3 - \text{Height}$$

The possible outcomes of the child’s obesity status can be broadly classified as

$$\text{Class 1 – Healthy} : \text{Class 2 – Obese} : \text{Class 3 – Indeterminate}$$

Using the three variables and outcome classes above, several observations are taken of children’s weight, age and height. Based on their obesity status, we can then have a decision tree as shown in Figure 2.4 below;

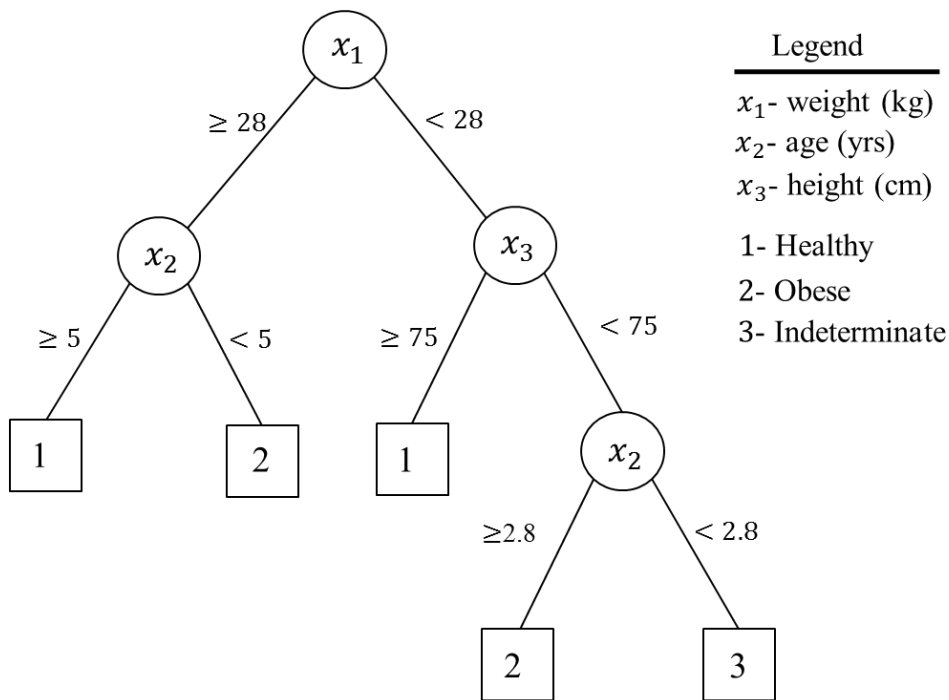


Figure 2.4: Decision Tree Example

The DT methodology is a nonparametric learning technique able to produce classifiers about a given problem in order to deduce information for new unobserved cases [11]. The DT has the hierarchical form of a tree structured upside down. The construction of a DT is based on a knowledge base (KB) consisting of a large number of operating points (OPs) covering all possible states of the power system

under study in order to ensure its representativeness. A vector of pre-disturbance steady-state variables, called attributes, characterizes each OP. The KB is divided in a learning set (LS) used for deriving the classifier structures and a test set (TS) used to evaluate the performance of these structures on new, unobserved OPs. The resulting decision tree can then be used to evaluate future operating conditions and predict the stability of a bus voltage based on the state of the attributes.

Decision trees have 3 main types of nodes;

- i. **A Root Node** – this exists at the top of the decision tree and represents the first split which affects all observations within the KB. The variable that appears at the root node is the variable with the greatest weight and effect on all the observations hence it is split first. In Figure 2.4, the root node has a split of x_1 at a value of 28kg.
- ii. **A Splitting / Decision Node** – these exist below the root node but are not terminal points. They represent split point in variables that occur as subordinate to the root node. They cascade down as the variables are split further and further into purer groupings. One variable can appear in several splitting nodes. In Figure 2.4, the node with a split for x_3 at 75cm is a decision node.
- iii. **Terminal Nodes** – these are the final points in the decision tree and represent the purest classification of a variable subsequent to the root and decision nodes. The path taken from the root node, through the decision nodes to the terminal nodes gives the set of splits undertaken in classifying the final variable appearing at the terminal node. In Figure 2.4, the terminal nodes are the ones with splits for x_2 at 5 years as well as the split for x_2 at 2.8 years.

In splitting all the variables in the KB according to their values, a split is done according to a predetermined algorithm. This algorithm can be determined in advance for small datasets where the values of the variables used to differentiate different classes in the observations KB are known. However, for large datasets with multiple variables, it is almost impossible to determine the split points.

As such, different heuristic algorithms have been developed which help in the splitting. These enable the observations to be classified starting at the root node and down through the decision nodes to the terminal nodes based on the relative values of the variables found in the observations. This further enables the sizing of the resulting decision tree by pre-determining either the minimum and maximum number of terminal nodes desired or determining the nodes based on the maximum allowable error within a root or decision node. In uni-variate discrete splitting (where only one variable is considered at a node), impurity criteria are used in determining the quality of a split, hence determining the value of a variable at a node that is used in splitting the observations. To determine impurity, if we have a variable x which has k discrete values distributed according to $P = (p_1, p_2, \dots, p_k)$, an impurity function can be formulated as $\emptyset: [0,1]^k \rightarrow R$ which must satisfy the following conditions [30];

- a) $\emptyset(P) \geq 0$
- b) $\emptyset(P)$ is minimum if $\exists p_i$ such that component $p_i = 1$ (minimum impurity occurs when one value has a probability of 1)
- c) $\emptyset(P)$ is maximum when $\forall i, 1 \leq i \leq k, p_i = 1/k$ (Maximum impurity is found when all values have equal probability distribution)
- d) $\emptyset(P)$ is symmetrical with regards to the components of P
- e) $\emptyset(P)$ is differentiable everywhere within its range

The quality of a split from a set of observations S is then determined relative to an attribute a_i as the reduction in the impurity of the attribute within the child nodes after the split. For instance, a node which has a class distribution $[0,1]$ has 0 impurity while a node with a class distribution $[0.5,0.5]$ has maximum impurity. Some common impurity measures include;

- i. **Information Gain / Entropy** – this criterion is also impurity based but employs an entropy measure as the impurity measure to check the quality of a split and aims at having a split that will maximise the entropy [31]. If at a node t there are c classes, the entropy at that node t can be defined as;

$$Entropy(t) = - \sum_{i=0}^{c-1} P(i|t) \log_2 P(i|t) \quad (2.11)$$

- ii. **Classification Error** – here the maximum error is calculated by looking at the split that will result in the purest split and comparing it with a perfect split where all observations are classified in one class [31]. It's defined as;

$$Error(t) = 1 - \max_i [P(i|t)] \quad (2.12)$$

- iii. **Gini Index** – The Gini index is a measure of impurity used to split nodes. It is calculated based on the number of observations belonging to one class at a node as a fraction of all the observations at that node. It is given by;

$$Gini(t) = 1 - \sum [p(j|t)]^2 \quad (2.13)$$

where $p(j|t)$ is the relative frequency of observations for class j at node t . The Gini index is maximum at $(1 - 1/n_c)$ when all observations are divided equally among all classes while it is minimum at 0 when all observations n at a node belong to one class c . The Gini index is then used to find the largest and purest partition at a node to ensure the observations are split in a way that reduces the chance of misclassifying an observation in a wrong class. A comparison of the 3 criterion is shown in Figure 2.5 below;

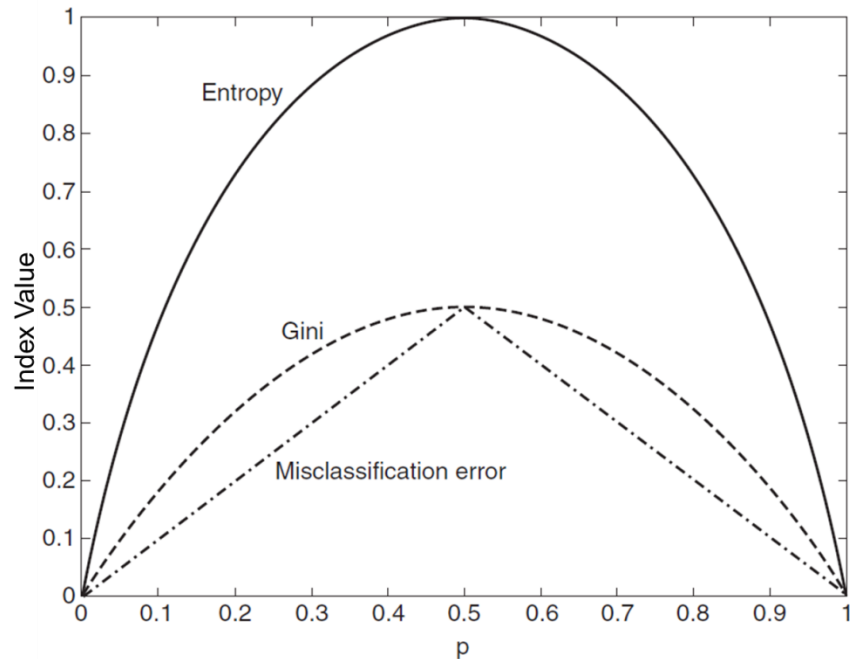


Figure 2.5: Comparison of DT Impurity Measures

Once the process of splitting nodes begins, it continues but must come to an end to prevent having an infinitely large tree. The criteria used to stop the splitting process is called the **Stopping Criterion**. This stopping criteria can be determined in several ways [30];

- i. When all observations belong to one single class
- ii. When the maximum tree depth has been reached in terms of levels of decision nodes
- iii. When the number of observations in a terminal node is less than the minimum number of observations set for a parent node hence that particular node cannot become a decision node.
- iv. When the number of observations in a child node would be less than the minimum number set for child nodes, even if the parent node has more than the minimum number of observations required.
- v. The splitting criteria to be applied is not greater than a set threshold.

There exist several ways of generating decision trees. These techniques result in the decision trees types classifications. The most common types of decision trees are given below;

2.6.3.1 ID3 Decision Trees

This type of tree uses the information gain impurity measure in the splitting [32]. The process of splitting is stopped when all observations belong to a single class or when the best value of information gain falls to below 0. Its main advantage is in the ease of construction but its biggest shortcoming is that it cannot be pruned to give trees with less leaf nodes if need arises.

2.6.3.2 C4.5 Decision Trees

This tree is a simple evolution from the ID3 tree [33]. It uses a modified gain criterion to split the observations and stops the stopping when any set criteria for stopping is reached. The main improvement is that it can be pruned to produce smaller trees. In addition, unlike the ID3 tree, the C4.5 tree can be used to handle purely numeric attributes and can induce missing observations or values from a given data set using the information gain criterion.

2.6.3.3 Classification and Regression Trees (CART)

Some situations arise where the input variables are known and a matching output is known as well. If very many instances of the input-output set exists, the relationship between the input variables and the outputs can be determined by performing a regression analysis on the variables. The output of this regression analysis indicates the correlation between each input variable and the output which is quantified as a weight. A decision tree is then constructed by splitting the input variables according to the weight and the range of the variable. In addition, CART involves a misclassification calculation so as to identify the variable to be split in the next level or whether the current splitting provides for a final node.

The process starts with the CART splitting the output based on a split using one variable only. It then evaluates the purity of the output using the single variable by using the Gini index and stores the heterogeneity score for that variable. It then repeats this process for all the variables. The variable that has the highest heterogeneity score is then considered the primary node and split first. The splitting then moves to the next level and continues with the splitting for the remaining variables. This form of regression and classification stops either when a desired level of heterogeneity is reached or when the number of splits specified is reached [34].

The last step is the pruning of the decision tree. If classification was done and a great number of nodes obtained, it may not be practical to work with a very large tree and so “pruning” of the tree is done. This involves reducing the number of splits and hence branches on the tree and evaluating what the error resulting from a miscalculation by having fewer splits would be. The smallest size of the tree that results in the lowest misclassification then becomes the optimum size of the pruned decision tree where a further decrease in the size of the tree results in a higher misclassification cost. This is because some variables may not be “costly” if misclassified in terms of the output as compared to others. The Gini index is most preferred in the misclassification computation [12].

The main advantage of CART over other decision trees is its ability to produce regression trees, hence being able to predict terminal values in terms of numbers not

just as classes. This ability is crucial in this research due to the need to predict bus voltages which will be in pu. values which are numbers.

Previously, decision trees have been used in data mining applications such as medicine for diagnosis of diseases [34] and in power systems for security studies [11] and more recently in voltage prediction [33] and voltage stability enhancement [35]. In this thesis, CART decision trees are used in the construction of decision trees for the buses within the IEEE 30 – Bus system and the Kenya Power System which are then used to predict the voltage magnitude and hence the voltage stability of load buses within the systems.

2.7 Previous Works

A weak bus can be defined as a bus within a power system that possesses the least capacity for increased reactive power demand during otherwise normal operations. Alammari [13] defines a weak bus as a bus that experiences a significant voltage and reactive power deviation for a small load change. Such a bus would then be very susceptible to voltage collapse in case of an increase in loading or a fault. Even if the fault occurs at a different bus connected to the weak bus through a transmission line, the weak bus would have a decreasing voltage magnitude, perhaps falling below feasible levels and causing either a brown-out or the protection system to isolate it as a fault. Identification of weak buses is critical as it enables system controllers to focus on the buses during peak loads and strained conditions and also provides a means for selecting optimized locations for FACTS devices.

Several methods have been used over the years to identify weak buses but artificial intelligence methods are the most popular in recent times. Alammari [13] used fuzzy logic in the identification of weak buses. In his paper, he develops a fuzzy logic algorithm with membership functions for the bus voltage and another for total reactive power demand at the bus. The fuzzy set so obtained by fuzzy multiplication of the two sets yields a decision set that is evaluated for each bus and used to classify the strengths of all the load buses.

Muriithi and Njoroge [14] used CPANN's to classify weak buses based on parameters from the Jacobian matrix used in load flow analyses. The procedure

involved performing multiple load flows with varying loading and contingency configurations and then using the resulting Jacobian values to train a CPANN network. The buses were then lumped together based on their voltage magnitudes for the various loading and contingency configurations to indicate their strength.

Cai and Erlich [15,16] used Singular Value Decomposition to perform dynamic voltage stability analysis on a 4-machine 2-area power system using a Multiple Input Multiple Output (MIMO) system. The system model included generator governor controls as well as SVC and STATCOM controllers. Voltage dependent loads were also included as well as the influence of tap changing transformers. They used the reduced Jacobian J_v to obtain the transfer function of the system for use in the MIMO system. The inputs came from controllers for real and reactive power at the generator and load buses while the outputs were the incremental bus voltages at all the buses in the system. The results indicated that generator AVR influence was highest in static stability while SVC controls have greatest influence when load modulation is introduced.

Ioannis and Konstadinos [17] performed dynamic voltage analysis by using multi-variable control theory with a MIMO system. Their work involved minimizing oscillations of state and network variables. This decoupled voltage stability from angle dynamics and assumed that all electromechanical oscillations are stable by use of the Eigen values of the voltage stability matrix. Their MIMO system had the system transfer function matrix using all generation and load controls as inputs and change in the voltage magnitudes at load buses as outputs.

Soni [18] used bifurcation analysis to perform voltage stability analysis. He considered changes in the system parameters with time which caused the stable equilibrium points at different loading levels to lose dynamic stability. This loss was caused by one of 3 bifurcations – singularity induced, saddle-node or Hopf bifurcations. He used Eigen value analysis to identify the bifurcation where the bifurcation is a sudden change in behaviour of the system as the system parameter passed through a critical value- the bifurcation point.

Cai et al [19] investigated the dynamic voltage stability of a system with the integration of a large wind farm. They used a MIMO system and analyzed stability by use of singular value decomposition of the reduced Jacobian. Further, they incorporated modal analysis to identify the critical oscillation modes. Their analysis was able to obtain the stability, controllability and participation indices for the system parameters.

Sun et al [20] performed dynamic security assessment using phasor measurements and decision trees. Their analysis involved simulation of a 24-hour period for the Entergy system and contingency analyses for n-1 and n-k probable contingencies. The results for all the operating conditions and contingency states were then used to train a decision tree using the Classification and Regression Tree (CART) algorithm. The decision tree was used to identify critical attributes from the system parameters that characterised the system's dynamic performance. Phase measurements of the critical attributes could then be compared to the decision tree to give the terminal node which indicated the insecurity score of the present operating condition.

Karapidakis and Hatziargyriou [21] used decision trees to construct an online based economic dispatch decision system for the island of Crete. Their research focused on balancing the cost of maintaining a spinning reserve big enough to maintain dynamic stability and meet any load changes with the cost of load shedding associated with loss of a generating unit due to stressed system operation occasioned by not having enough spinning reserve. The costs were calculated with various generation mixes to develop a decision tree that could be used for online determination of the optimum generation mix for any given loading condition.

Subramani et al [22] used a line stability index to classify weak and critical lines in the IEEE Reliability Test System. They developed a line outage contingency index as a predictor of voltage stability since line outages contribute greatly to voltage instability. The index was then tested for different loading conditions in order to identify what effect increased loading would have on the voltage stability during critical line outages and thereafter rank weak areas within the system. Their research

also yielded a contingency ranking based on the line outage index as an indicator of voltage stability.

Izzri et al [23] used a Power Transfer Stability Index as an online based indicator of distance to voltage collapse. The PTSI was constructed using an RBFNN using training data from various loading and contingency conditions on the Iraqi Super Grid Network. The input variables consisted of bus voltages, real and reactive power demand at each bus and generator load angles for the RBFNN. The resulting index then makes it possible to automatically classify critical buses based on loading and contingency conditions of the system on an online basis since the parameters can be measured using a SCADA system. In their research, the classification using the PTSI was faster than the use of a Back Propagating Neural Network in classification of critical buses for the same data, showing the superiority of the index compared to the traditional load flow.

Kumaraswamy et al [24] used the L-index in calculating an optimal power flow on the IEEE 6-bus and IEEE 9 - Bus test systems. The L-index was constructed from the basic Kirchoff's laws as applied in the Y-bus matrix as shown in equation (2.14) below;

$$L_j = \left| 1 + \frac{V_{0j}}{\bar{V}_j} \right| = \left| \frac{S_j + S_{jcorr}}{Y_{jj+}^* \cdot V_j^2} \right| \quad (2.14)$$

where

$$V_{0j} = - \sum_{i=1}^{NG} F_{ji} \cdot \bar{V}_i \quad (2.15)$$

$$S_{jcorr} = \left(\sum_{\substack{i=1 \\ i \neq j}}^{NLB} \frac{Z_{ji}^*}{Z_{jj}^*} \cdot \frac{S_i}{\bar{V}_i} \right) \cdot \bar{V}_j \quad (2.16)$$

with

$$Y_{jj+} = \frac{1}{Z_{jj}}$$

F_{ji} is the ji^{th} element of the Objective Function Matrix

Z_{jj} is the jj^{th} element of the impedance matrix

S_i is the complex power demand at bus i

\bar{V}_i is the bus voltage at bus i

NG is the total number of generator buses

NLB is the total number of Load buses in the system

From the voltage stability index L , they were able to relate the increase in loading condition with the index and use it as a predictor of voltage collapse. The L -indicator is applicable in both static and transient conditions and so provides a powerful tool for both static and dynamic analysis.

2.8 Conclusion

From the techniques and areas highlighted in this chapter, the following were adopted for this research;

- i. The type of voltage stability to be investigated would be Dynamic Voltage Stability. This dynamic nature of the analysis would be achieved by taking numerous load variations while tracking the changes in voltage so as to simulate the changes in the voltage magnitudes at the load buses with changes in loading and line contingencies.
- ii. Only one type of contingency, a single – line outage, would be studied at a time in order to limit the scope of the research.
- iii. The VCPI index was selected for use in this research. This was due to the fact that it is calculated for load buses and not lines and so would only require to be calculated once for a load bus unlike the line indices that are calculated many times for a single bus. Also, the variables required for its calculation are easily retrievable after a load flow.
- iv. The CART decision tree was selected as the type of artificial intelligence for study in the research. This was due to the fact that the Gini index used to

calculate the error at each classification split reduces the probability of erroneous classification of observations. In addition, the CART trees have the ability for classifying observations and predicting numerical terminal nodes, instead of using classes. This was critical to the research as they could then be used to predict voltage magnitudes at a bus. Also, CART trees carry an inherent ability to produce regression trees and be pruned to several levels.

- v. The IEEE 9 – Bus and 30 – Bus systems were selected for validating the various developed algorithms. The IEEE 9 – Bus is a relatively small system which enabled the development and debugging of the algorithms while the IEEE 30 – Bus was similar in size to the Kenya Power System – 1996 Model which has 37 buses.
- vi. The MATLAB © software was used for simulation in this research. Specifically, the R2010 version, 32-Bit MATLAB software was used. An addition of the Power System Toolbox developed by A. Sadaat was incorporated to enable the performance of Load Flow studies. MATLAB was selected because it enables the creation of user defined codes for variations of various parameters during the simulation. In addition, MATLAB has an inbuilt CART creation model within its Statistics Toolbox, as well as an inbuilt Artificial Neural Network toolbox which enables the creation, training and deployment of ANNs. The addition of the Power System Toolbox which has load flow calculations inbuilt also made the retrieval of the load flow results possible. MATLAB also has an ability to export and import data to Microsoft Excel documents, which was instrumental in storing the results. The software was run on a computer running a 32 bit version of Microsoft Windows 7 operating system with a 2.8GHz processor and 4GB of RAM.

CHAPTER THREE

METHODOLOGY

3.1 Introduction

In this chapter, the Kenya Power System in appendix A4 is analysed using the CART method during the dynamic voltage stability analysis. The Kenya Power System has 37 buses.

The contingency considered involved a single – line outage for each of the 38 lines in the Kenya Power System

In the Kenya Power System, the parameters of interest are;

- i. P – the Active power demand at all the buses within the system
- ii. Q – the reactive power demand at all the buses within the system
- iii. K – the single line outage
- iv. $J_1 = \frac{\partial P}{\partial \theta}$ the partial derivative of the active power with respect to the pf at a bus
- v. $J_3 = \frac{\partial Q}{\partial \theta}$ the partial derivative of the reactive power with respect to the p.f. at a bus

The Kenya Power System model used in the 1996 model which has 37 buses and 38 lines. The IEEE 30 – Bus test system was used for validation of the VCPI and CART algorithms by virtue of being close in terms of bus number to the Kenya Power System. The Newton – Raphson power flow solution method was used for performing the power flow analysis. The one-line diagram as well as the base case values for the IEEE 9 – Bus, IEEE 30 – Bus and the Kenya Power systems are described in detail in the Appendix section. For uniformity, the base MVA was selected as 100MVA for all the systems.

In performing the dynamic voltage stability analysis of the Kenya Power System, the following steps were followed;

3.2 Verification of VCPI Parameters - IEEE 9 – Bus System

Using the IEEE 9 - Bus system in Fig. 3.1 below, a load flow study was carried out on the system using the base case system values. The detailed system model is given in appendix A1.

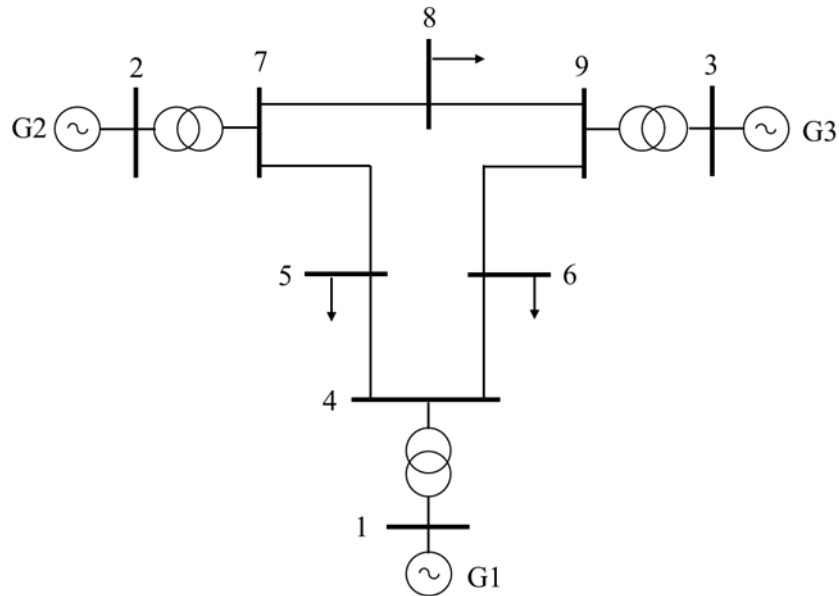


Figure 3.1: IEEE 9 – Bus System

Since bus 5 had previously been identified as the weakest bus in the system [24], the loading on Bus 5 was increased in steps of 0.001pu while maintaining power factor until when the power flow solution failed to converge. At each loading step, the VCPI index was calculated and the results of the VCPI and voltage magnitude at bus 5 were then compared with those from literature. The procedure is detailed in Figure 3.2 below;

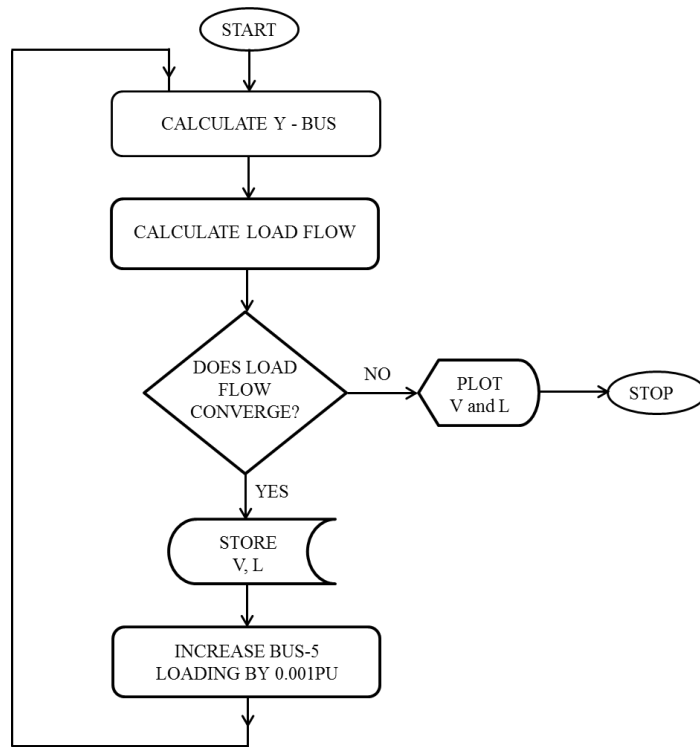


Figure 3.2 : VCPI Calculation Algorithm for IEEE 9 - Bus (Bus 5)

The results of the procedure were then compared with those from literature in order to validate the calculation of the VCPI for incremental loading.

3.3 Application of VCPI with ANN - IEEE 30 – Bus System

Next the IEEE 30 - Bus system as shown in Figure 3.3 was studied. The detailed system model is given in appendix A2.

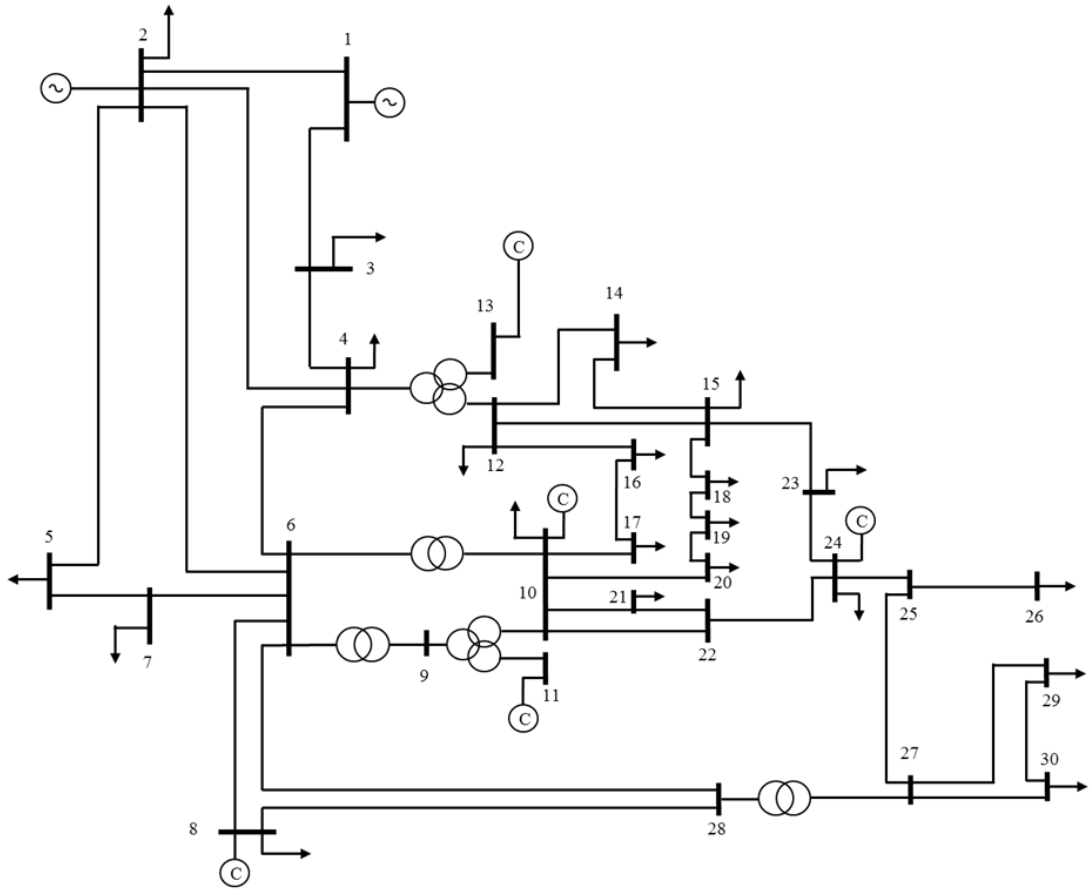


Figure 3.3: IEEE 30 – Bus System

This involved iterations for the base case and with an $n - 1$ contingency. The contingencies were selected as single – line outage and for transformers the tap settings were varied between 90% and 110% of the nominal tap setting, which is the maximum variation of the transformer tap possible. For each line contingency and the base case system values, 100 random loading configurations of between 30% and 200% at each load bus were done without maintaining power factor. The randomization of the load was done in order to simulate dynamic operating conditions. The maximum and minimum load setting was varied in order to capture overload conditions and light loading conditions as well. Within each of these nested iterations, a load flow study was run with the single line outage and load configuration. From the load flow, the voltage magnitudes, real and reactive power at each bus and for the whole system were recorded. The L – index was then calculated for that configuration. This data was then used to train an ANN with 100 neurons in

the hidden layer. The ANN used had 5 inputs for the following inputs $P_{26}, P_{NET}, Q_{26}, Q_{NET}, k$ representing the real power demand at bus 26, total real power demand in the whole system, reactive power demand at bus 26, total reactive power demand in the whole system and the line contingency respectively. It had 2 outputs for the voltage magnitude and VCPI index at bus 26. The training method used was Levenberg-Marquardt using the mean squared error with 70% of the sample used for training, 15% for validation of the network and 15% for testing the final network. Each epoch was limited to a maximum of 1000 iterations and 6 validation checks were performed. Previous studies [14] found bus 26 to be the weakest bus in the system. A comparison of the VCPI calculated from the Power Flow and that predicted by the ANN was then carried out using a separate set of loading and contingency snapshots for the system to determine the dependability of the VCPI index with varying loading and contingencies, and the effect of the real and reactive power demands at the weak bus and in the whole system. The procedure is detailed in Figure 3.4 below. The IEEE 30 - Bus system has 41 lines.

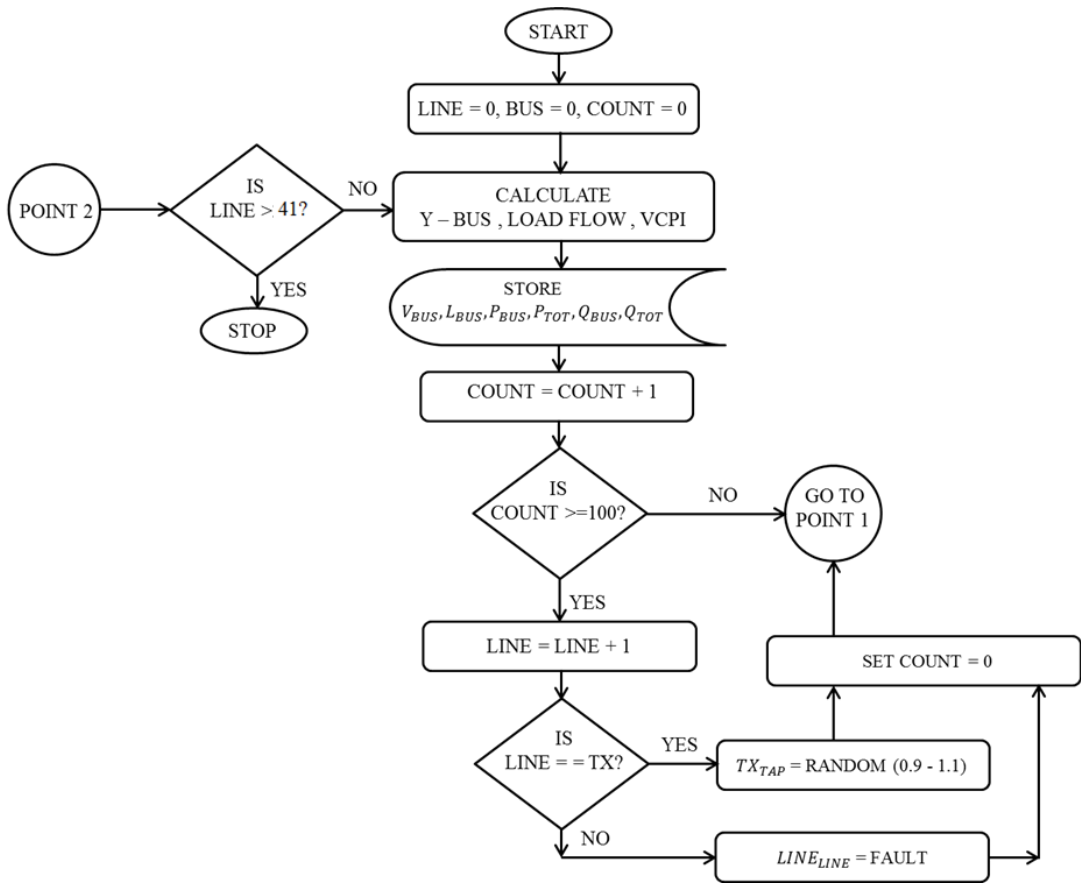


Figure 3.4(a): VCPI – Line Contingency Simulation

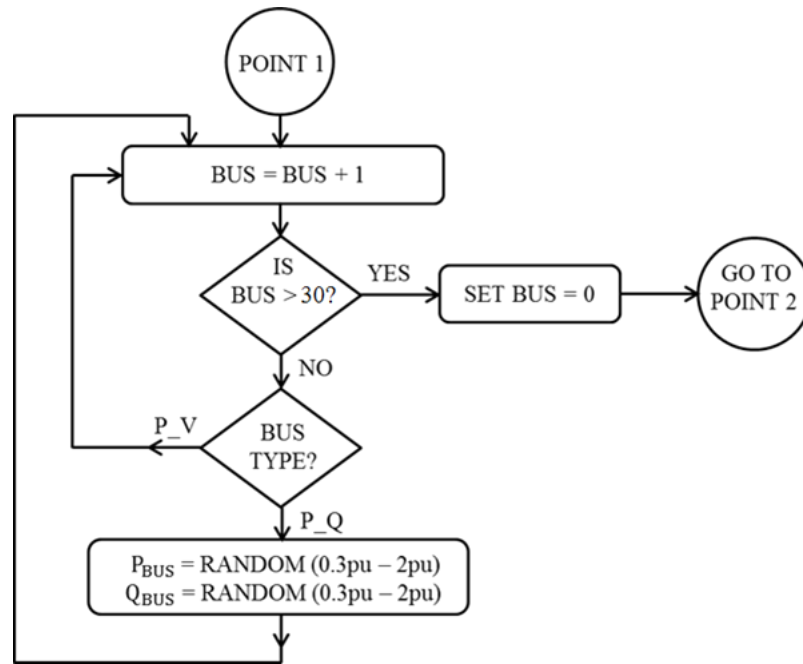
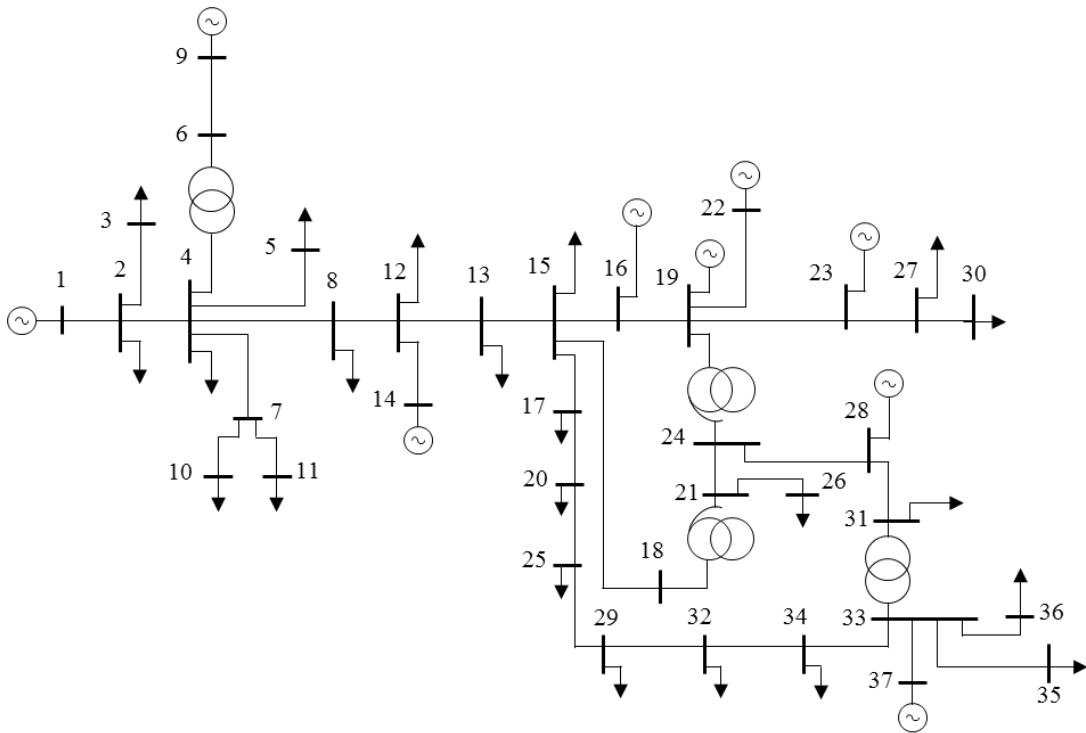


Figure 3.4(b): VCPI - Bus Loading Variation

3.4 VCPI with ANN Based Analysis - Kenya Power System

Based on the results from the IEEE 9 - Bus and IEEE 30 - Bus system and the algorithm developed for the ANN for predicting VCPI, the study in section 3.2 was repeated on the Kenya Power System as shown in Figure 3.5 below. The detailed system model is given in appendix A3.



Bus No	Location	Bus No	Location	Bus No	Location	Bus No	Location
1	Tororo	11	Chemosit	21	Dandora	31	Rabai
2	Musaga	12	Naivasha	22	Gitaru	32	Mangu
3	Webuye	13	Ruaraka	23	Masinga	33	Rabai
4	Lessos	14	OIKaria	24	Kamburu	34	Mariakani
5	Eldoret	15	Juja	25	Mtito Andei	35	Kilifi
6	Lessos	16	Kin daruna	26	Embakasi	36	Bamburi
7	Muhoroni	17	Sultan Hamud	27	Kiganjo	37	Kipevu
8	Lanet	18	Dandora	28	Kiambere		
9	Turkwell	19	Kamburu	29	Voi		
10	Kisumu	20	Kiboko	30	Nanyuki		

Figure 3.5: Kenya Power System

A previous study [14] had identified buses 10, 22, 30 and 31 as the weakest buses within the system and so the study focused on bus 10 and 30. Bus 22 is a generator bus and bus 31 is a node bus having no load connected to it hence they were ignored. 100 iterations of load flows were conducted each with the loads at each load bus varied by between 50% and 150% of the nominal value for each contingency, in order to simulate light loading and overloading conditions. Increasing the loading margin of the Kenya Power System below 50% and above 150% led to the non-convergence of the load flow hence the loading was limited to 50% - 150%. This is

due to the fact that the Kenya Power System data is ill-conditioned and not as optimised as the IEEE 30 – Bus system data, especially for experimental analysis. For each loading-contingency configuration, a load flow calculation was performed and each bus voltage and VCPI for each bus calculated and stored. The results were used to train an ANN. The ANN was used to predict the VCPI using a separate generated set of loading and contingency contingencies. The results for the calculated VCPI values and those from the ANN were then compared for the 2 weak buses. The procedure is detailed in Figure 3.6 below. The Kenya power system has 37 buses and 38 lines;

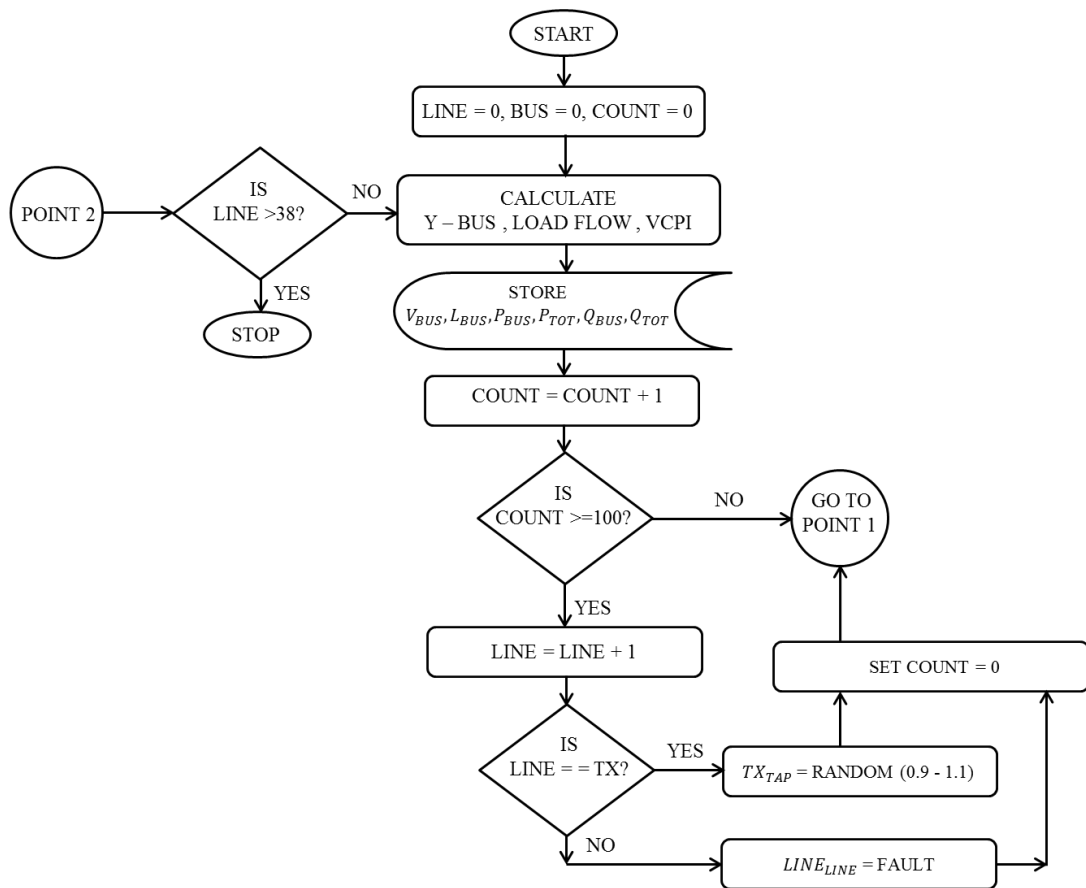


Figure 3.6 (a): VCPI Application - Kenya Power System – Load Flow Calculation

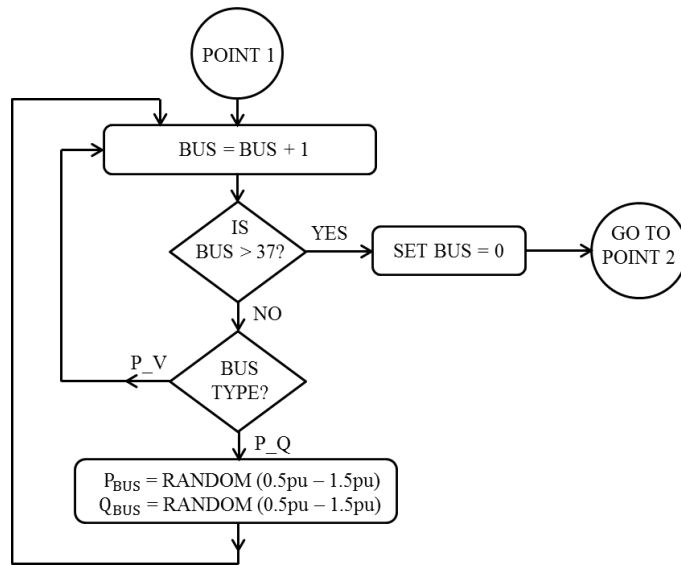


Figure 3.6 (b): VCPI Application - Kenya Power System – Load Variation

In the second set of simulations, the loading at each weak bus was increased, while maintaining power factor and the power at all other buses at their nominal value, until the voltage magnitude dropped to 0.9pu at the weak bus. The VCPI was obtained at the point which coincided with the voltage magnitude being 0.95 in order to obtain the VCPI at the minimum allowable voltage level of 95% in the Kenya power system. The procedure was repeated for the 2 weak buses. The procedure is detailed in Figure 3.7 below.

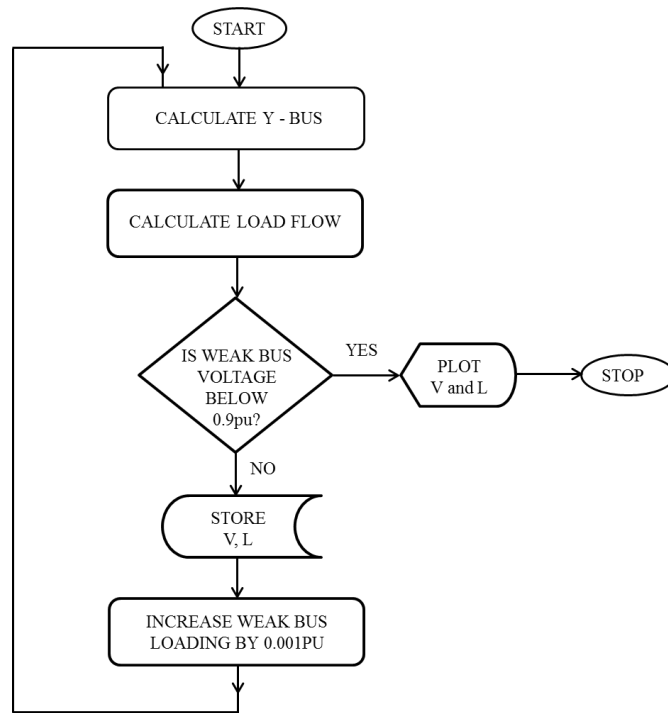


Figure 3.7: VCPI at 95% Weak Bus Voltage Drop – Kenya Power System

3.5 Developing of CART Algorithm – IEEE 30 – Bus System

A similar algorithm to the one used in the VCPI with ANN training in section 3.2 was used. The iterations were done for the base case and for the case with an $n - 1$ line contingency. The contingencies were selected as single – line outages and for transformers the tap settings were varied between 90% and 110% of the nominal tap setting. For each contingency configuration, 100 random loading configurations of between 50% and 150% of the base case values at each load bus were done without maintaining power factor. Within each of these nested iterations, a load flow study was run with the single line outage and load configuration. From the load flow, the following variables were recorded and stored for each load bus j ;

P_i – Real Power Matrix for configuration i

Q_i – Reactive Power Matrix for configuration i

Y_{jj} – The jj^{th} Element in the $Y - bus$ matrix

K_i – The contingency location

J_{1j} – the j^{th} element in the J_1 matrix from the Jacobian

J_{3j} – the j^{th} element in the J_3 matrix from the Jacobian

P_i and Q_i were the vectors for all the real and reactive power supplies at all the buses within the system corresponding to the load-contingency configuration after the load flow calculation.

The 6 variables formed the inputs used in construction of the CART tree. The bus voltage obtained at bus j after the power flow iteration formed the target output for the Decision Tree. The minimum number of variables set for observation was set at 3000. This number of observations was set so as to achieve a decision tree that wasn't too small such as to draw very wide conclusions or too large as to make it difficult to read. Cross validation using the Gini index was used in pruning the tree and obtaining the minimum cost tree.

The study focused on bus 26 in the IEEE 30 - Bus system, which had previously been identified as the weakest bus in the system [14]. Once the complete tree had been constructed, the minimum – cost tree was plotted. For analysis purposes, the pruning level of the decision tree was increased by 1 in order to have a CART decision tree with more than 1 node. This was also plotted. The procedure is detailed in Figure 3.8;

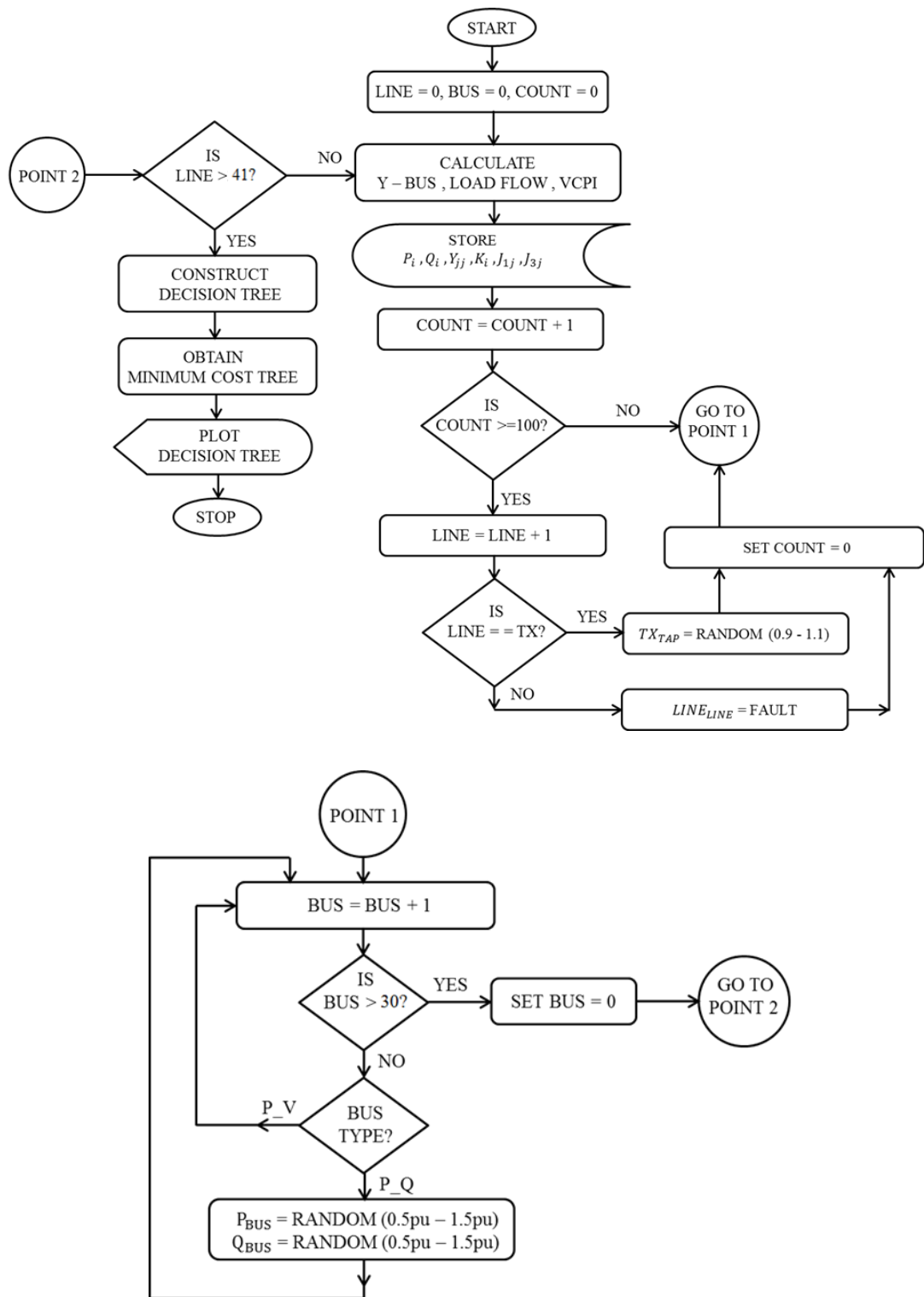


Figure 3.8: CART Construction Algorithm – IEEE 30 – Bus System

3.6 CART Based Analysis - Kenya Power System

Using the algorithm developed with the IEEE 30 – Bus system, CART decision trees were constructed for the Kenya power system. The steps involved were the exact ones used in the one for the IEEE 30 – bus system except for the number of buses and lines. The Kenya Power System has 37 buses and 38 lines. The study focused on the 2 weak load buses within the system, buses 10 and 30. The procedure is detailed in Figure 3.9;

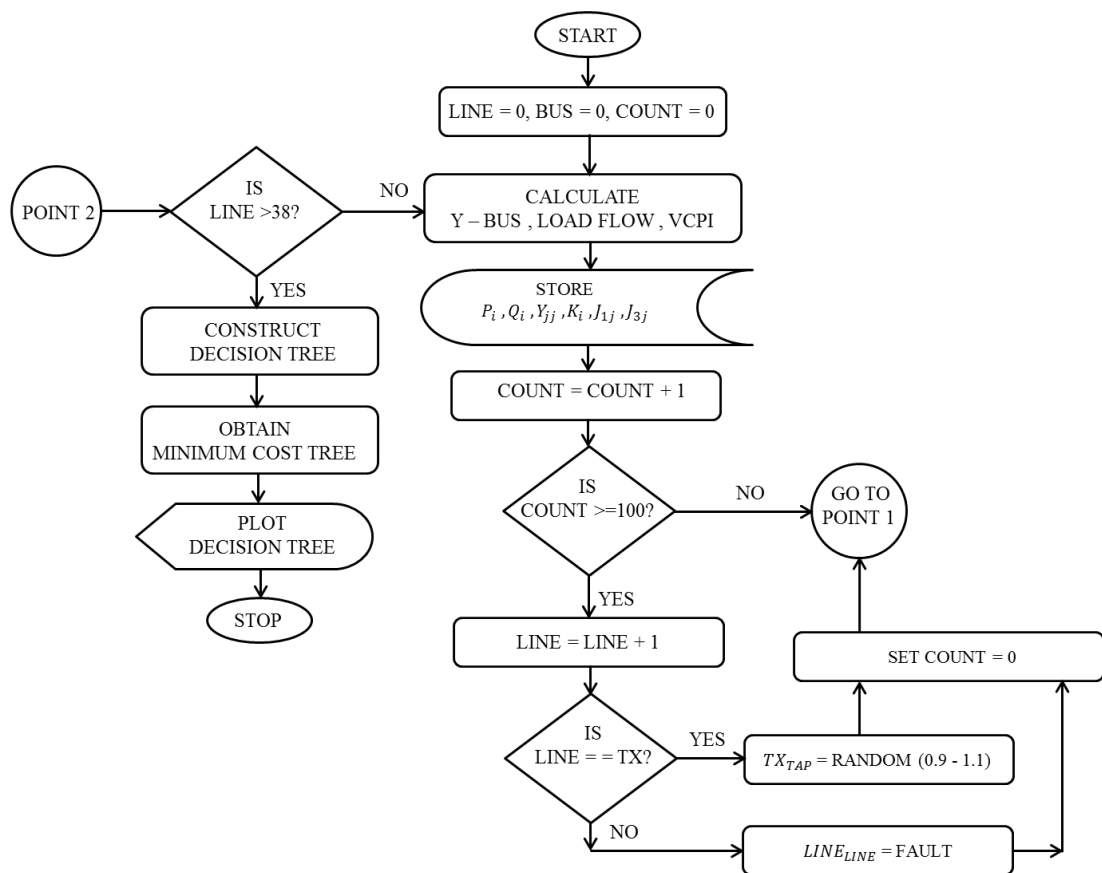


Figure 3.9(a): CART Construction Algorithm – Kenya Power System – Load Flow Calculation

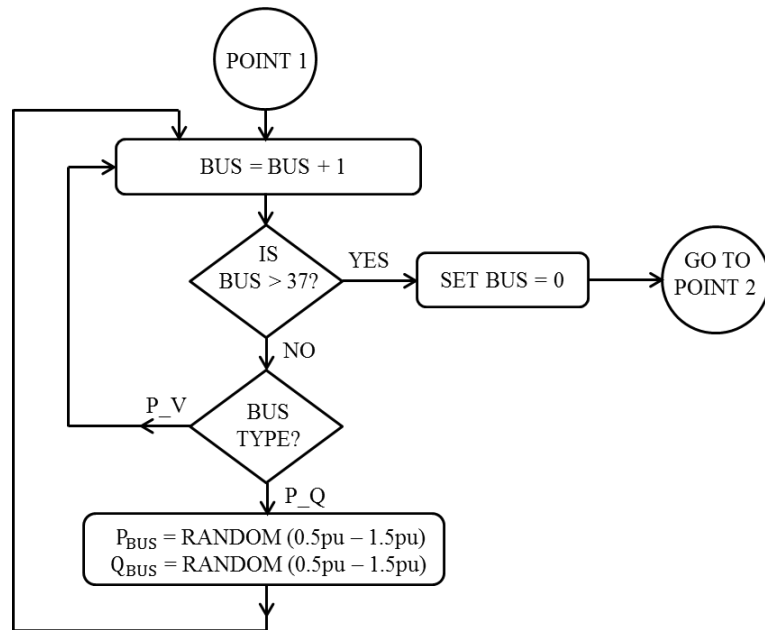


Figure 3.9(b): CART Construction Algorithm – Kenya Power System – Load Variation

3.7 Conclusion

In this chapter, a detailed description of the steps followed in undertaking the research leading to the thesis is given. The steps involved verification of the VCPI calculation algorithm and testing it on the IEEE 9 – Bus system. This was followed by testing of the predictive capacity of an ANN for the VCPI index and testing it on the IEEE 30 – Bus system. After that, the CART development algorithm is described and tested on the IEEE 30 – Bus system before being applied to the Kenya Power System.

CHAPTER FOUR

RESULTS AND ANALYSIS

4.1 Introduction

In this chapter, the results focus on the application of VCPI with ANN for the IEEE 9 – Bus test system, development of an algorithm on application of VCPI with ANN to the IEEE 30 – Bus system and analysis of the same for the Kenya Power System.

Based on the results of the above, a CART algorithm for the IEEE 30 – Bus system is developed and applied on the Kenya Power System.

4.2 Verification of VCPI Parameters - IEEE 9 – Bus System

Using the IEEE 9 - Bus system, the loading in bus 5 was increased starting from Op.u. until when the load flow calculation using the Newton-Raphson iterative method failed to converge, while maintaining power factor at the base case value. The corresponding values of the voltage magnitude and VCPI values were then plotted against the loading as shown in Figure 4.1

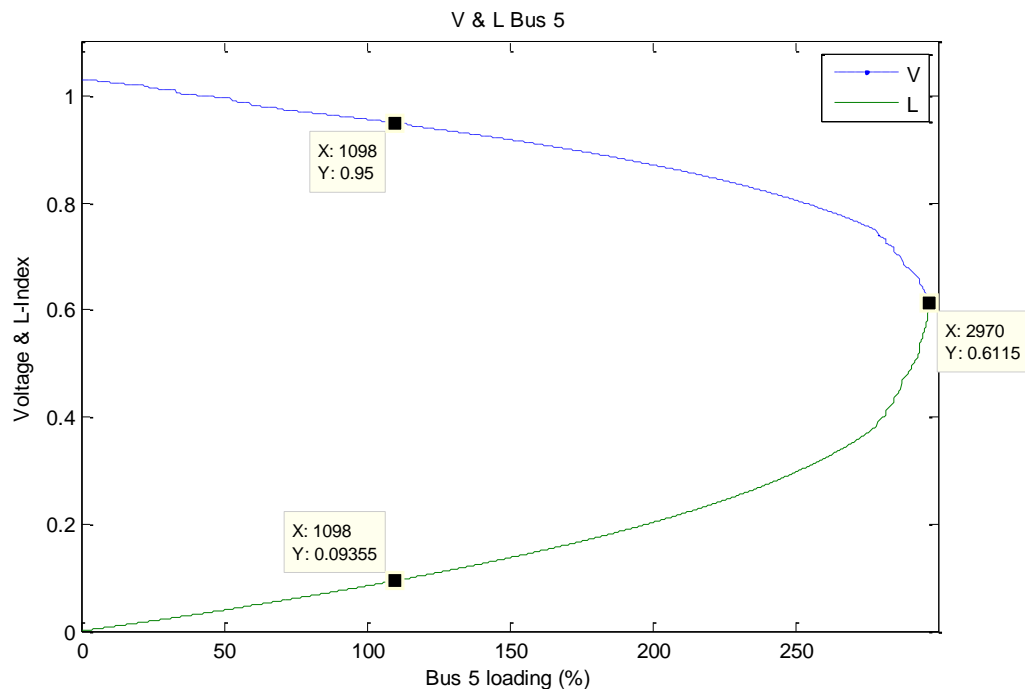


Figure 4.1: VCPI and Voltage at bus 5 for bus 5 loading – IEEE 9 - Bus System

This result matched previous studies using the VCPI [24] with the non-convergence of the load flow for Bus 5 occurring at 2.971pu (371+j149MVA). The curve for the voltage magnitude follows the general PV curve shape with the voltage magnitude decreasing with the increase in power demand. The curve for the VCPI index is inverse of the voltage magnitude and increases with increase in the power demand at bus 5. The results showed that the voltage at bus 5 would drop to 0.95 pu when the loading was at 1.09pu based on the base case values. This result validated the code used in the calculations of the VCPI. The load in bus 5 was increased in steps of 0.001p.u. hence in Figure 4.1 the x-axis indicates the percentage load.

4.3 Application of VCPI with ANN - IEEE 30 – Bus System

To take into account the effect of the loading on all the other buses, the second algorithm was developed and applied on bus 26. It involved creating single line outage and then varying the loading on each bus randomly between 0.5p.u. and 1.5p.u., in order to mimic realistic loading conditions, and then calculating a load flow with this load-contingency configuration. For lines which were transformers, the tap position was randomly varied between 90%-110%. From the load flow, the VCPI at bus 26 was calculated. For each contingency, 100 random loading configurations were performed. The resulting data was then used to train an ANN and a comparison between the data generated by the calculated load flow and the ANN were compared as shown in Table 4.1;

Table 4.1: Comparison of VCPI using Load Flow and ANN (Bus 26 – IEEE 30 - Bus System)

All values in (pu)					VCPI		
					METHOD		Error (pu)
P_{26}	Q_{26}	P_{tot}	Q_{tot}	Line outage	Calculated	ANN	
1.03	0.68	0.802	0.977	18	0.017716343	0.017671996	0.00004
1.31	0.75	0.795	0.836	4	0.022009059	0.022171478	0.00016
0.55	1.07	0.893	1.022	8	0.014192884	0.014241535	0.00005
1.25	0.7	0.900	1.160	4	0.021715184	0.021684374	0.00003
0.94	1.18	0.898	0.809	25	0.0196072	0.019471719	0.00014
0.98	1.34	0.832551	1.022147	34	0.021028836	0.021253513	0.00022
1.03	1.34	0.973613	1.170182	27	0.022764464	0.022584672	0.00018
0.56	0.56	0.973737	0.973296	17	0.010444373	0.010501276	0.00006
0.97	1.34	1.053596	0.914952	1	0.02089014	0.021338839	0.00045
1.15	1.4	1.07819	1.058376	11	0.024649791	0.024517657	0.00013
1.5	1.08	0.924584	1.202393	17	0.027959071	0.027665566	0.00029
1.03	1.28	0.918574	0.874635	39	0.02153542	0.021375219	0.00016
1.3	0.85	0.903493	0.983185	38	0.022614455	0.022791696	0.00018
1.36	0.79	0.921351	0.965	39	0.023441694	0.023538126	0.00010
1.15	1.23	1.054414	0.932005	24	0.022850865	0.022853261	0.00000
0.73	0.76	1.227085	0.800697	33	0.014181215	0.014141223	0.00004
0.92	1.45	0.831189	1.040158	34	0.021552404	0.021524221	0.00003
1.35	1.19	1.212689	1.079501	8	0.026614541	0.026526106	0.00009
0.62	0.65	0.763278	0.959643	15	0.011803074	0.011804038	0.00000
1.03	1.19	0.913342	0.99874	16	0.020926418	0.020901713	0.00002

From Table 4.1, the ANN is capable to predict the VCPI values to an accuracy of above 99%. This concurs with the results from [25] which are given in appendix A4. Also, it shows that the VCPI doesn't have to be calculated directly from the load

flow which means an online system can be used to predict VCPI values based on power demand parameters which can be read online from a SCADA system.

4.4 VCPI with ANN Based Analysis - Kenya Power System

To begin with, the loading at each individual weak bus was increased in steps of 0.001p.u. and the effect on the voltage magnitude and VCPI was recorded as seen in Figure 4.2 and Figure 4.3 for bus 10 and Figure 4.4 and Figure 4.5 for bus 30.

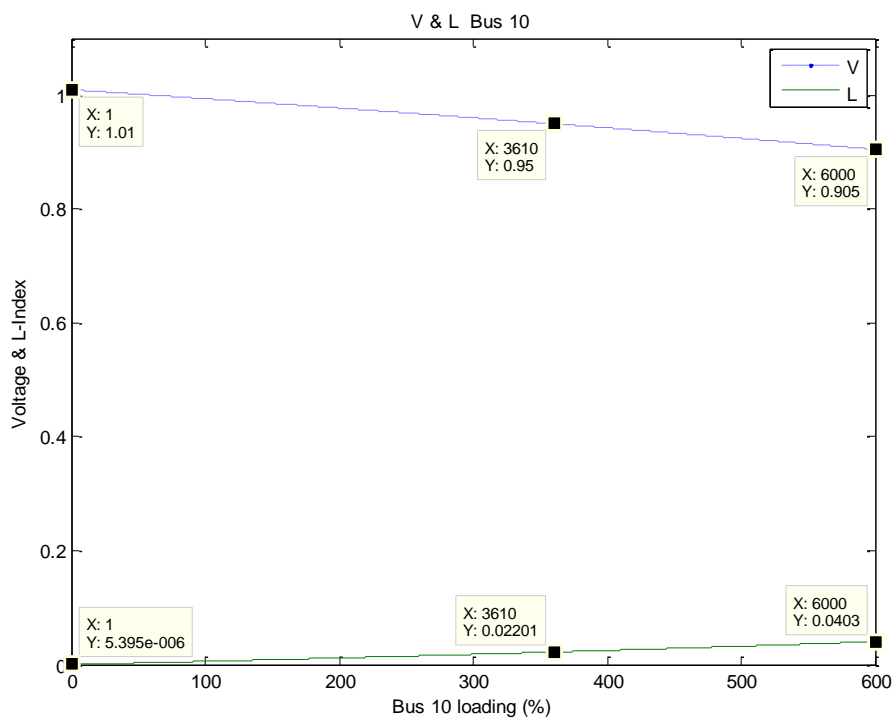


Figure 4.2: VCPI and Voltage at bus 10 for bus 10 loading – Kenya Power System

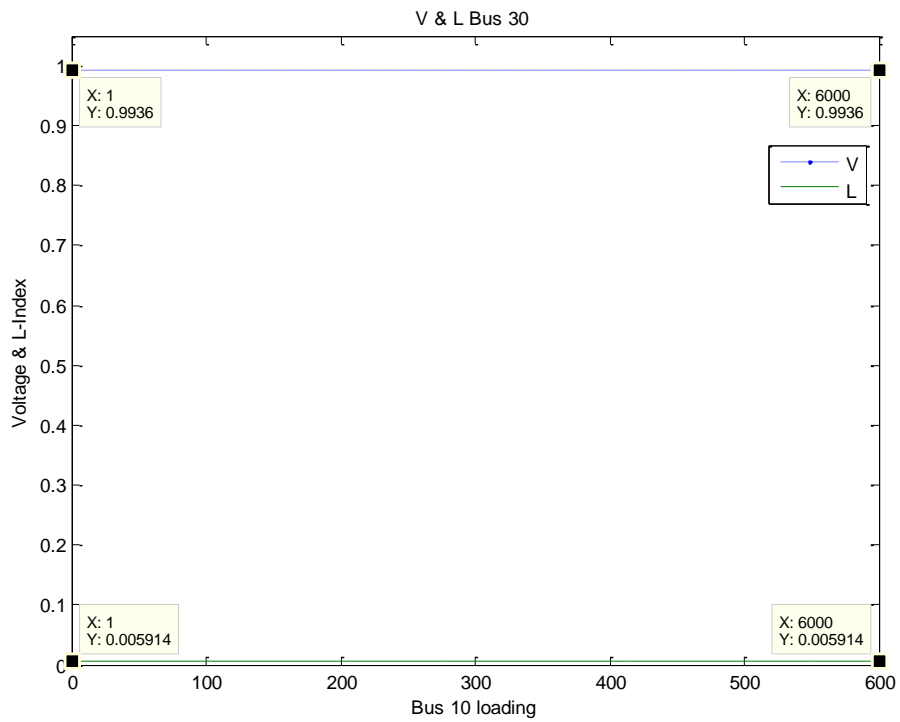


Figure 4.3: VCPI and Voltage at bus 30 for bus 10 loading – Kenya Power System

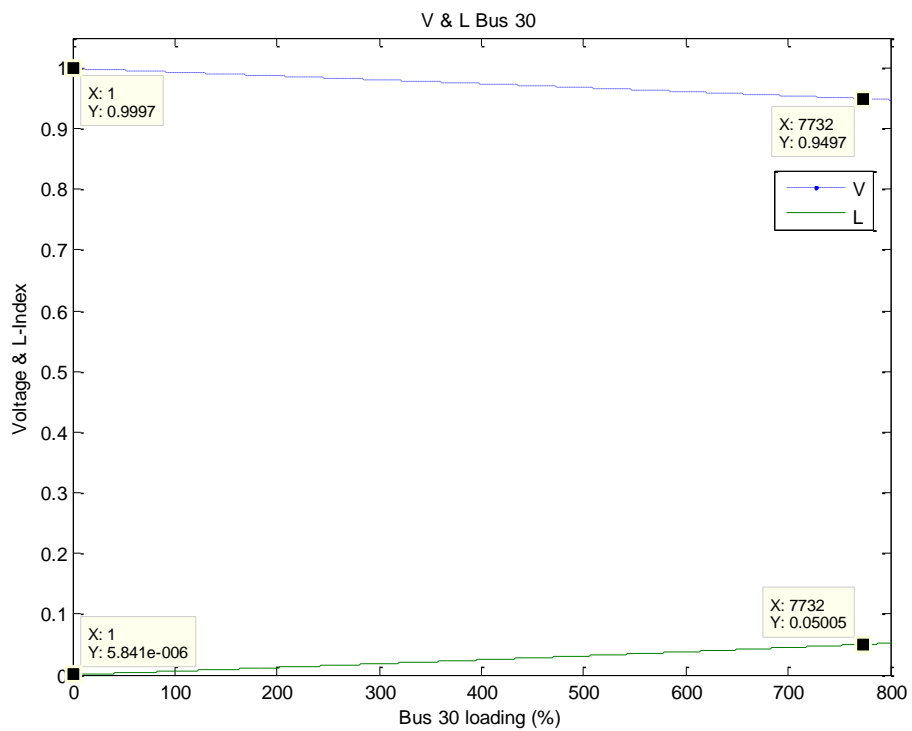


Figure 4.4: VCPI and Voltage at bus 30 for bus 30 loading – Kenya Power System

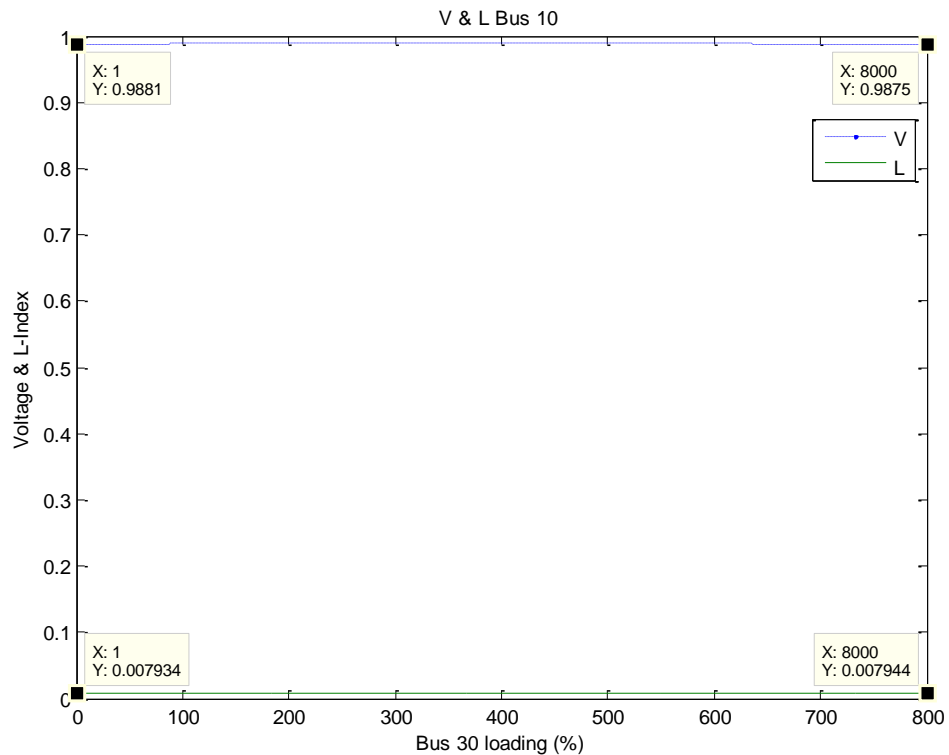


Figure 4.5: VCPI and Voltage at bus 10 for bus 30 loading – Kenya Power System

For loading on bus 10, the voltage magnitude and VCPI at bus 10 show a correlation with the VCPI increasing as the voltage magnitude reduces until 0.905p.u. when the loading is 6p.u.on bus 10 with the loading on all other buses maintained at the nominal level. For bus30, the physical and electrical distance between them makes the effect on the loading on bus 10 insignificant. Bus 30 (Naivasha) is approximately 500 km away from bus 10 (Kisumu) with many nodes in between them. This explains why the loading on bus 10 has little effect on the voltage and VCPI at bus 30.

For loading on bus 30, a similar effect to that from bus 10 loading is experienced. The voltage magnitude and VCPI at bus 30 are affected by the loading but bus 10 not significantly affected.

To simulate multiple loading conditions, the algorithm in section 3.3 was applied to the Kenya Power System with one ANN being trained for bus 10 and another for bus 30. A comparison of the VCPI values generated by calculating a load flow and by

use of a ANN were compared as seen in Table 4.2 for bus 10 and Table 4.3 for bus 30 below;

Table 4.2: Comparison of VCPI using Load Flow and ANN (Bus 10 – Kenya Power System)

All Values in (pu)					VCPI		
					Method		Error (pu)
P_{10}	Q_{10}	P_{total}	Q_{total}	Line outage	Calculated	ANN	
1.11	0.64	1.024	1.057	11	0.008598	0.008598	0.000000
1.15	0.6	0.992	0.954	18	0.008881	0.008879	0.000002
1	1	1.000	1.000	0	0.007928	0.007924	0.000004
0.61	1.42	1.158	0.926	21	0.005605	0.005609	0.000004
0.63	0.92	0.812	0.843	10	0.00517	0.005164	0.000006
0.63	0.6	0.980	0.925	22	0.004878	0.004886	0.000007
0.87	1.46	1.074	0.736	20	0.007326	0.007315	0.000011
1.36	1.27	1.248	1.092	27	0.011108	0.011119	0.000011
0.74	1.27	1.054	1.112	16	0.006293	0.006282	0.000012
0.55	0.64	1.070	1.111	24	0.004362	0.004377	0.000015
0.73	0.78	1.022	0.888	35	0.005785	0.005768	0.000017
0.69	1.26	1.070	1.051	6	0.005961	0.005937	0.000024
1.08	0.94	1.022	1.187	33	0.008514	0.00854	0.000026
0.67	1.01	0.978	0.965	13	0.005542	0.005515	0.000028
0.81	0.86	0.945	0.956	26	0.00642	0.006392	0.000028
0.55	1.41	0.882	0.744	1	0.005113	0.005143	0.000030
0.8	1.21	0.900	1.181	31	0.006681	0.006651	0.000030
1.08	0.73	0.921	0.790	20	0.008368	0.008402	0.000034
0.95	1.15	1.008	1.092	33	0.007703	0.007669	0.000034
0.88	1.36	0.981	0.900	1	0.007308	0.007342	0.000034

Table 4.3: Comparison of VCPI using Load Flow and ANN (Bus 30 – Kenya Power System)

All Values in (pu)					VCPI		
					Method		
P_{30}	Q_{30}	P_{total}	Q_{total}	Line outage	Calculated	ANN	Error (pu)
1	1	1.039369	1.119826	10	0.005914	0.005914	0.00000001
1.33	1.25	1.02525	1.126762	20	0.007809	0.007809	0.00000003
1.44	0.76	0.89508	0.976154	11	0.00794	0.00794	0.00000004
1	1	1	1	0	0.005914	0.005914	0.00000004
0.62	0.71	1.021315	0.98173	17	0.003757	0.003757	0.00000004
0.54	0.94	1.022036	0.957835	14	0.003741	0.003741	0.00000006
0.96	1.25	0.941386	1.200582	38	0.006042	0.006042	0.00000017
0.73	1.49	1.062345	0.942928	30	0.005455	0.005455	0.00000018
0.73	0.64	0.838208	1.085164	14	0.004206	0.004206	0.00000018
1.04	0.67	1.111917	0.927714	3	0.005796	0.005796	0.00000018
0.75	0.78	0.964976	0.959773	36	0.004457	0.004456	0.00000020
1.27	0.94	1.228703	1.010434	32	0.007199	0.007199	0.00000021
1.37	1.04	0.875861	0.959267	9	0.007798	0.007798	0.00000021
1.47	0.66	1.119349	0.950884	29	0.008036	0.008036	0.00000024
0.67	0.8	1.014636	1.104771	23	0.004104	0.004104	0.00000028
0.55	1.07	1.034707	0.907257	33	0.004005	0.004004	0.00000028
0.57	1.21	0.929119	0.954326	38	0.004334	0.004334	0.00000029
0.58	1.13	1.150198	1.008111	9	0.004228	0.004228	0.00000030
1.27	1.28	1.039261	1.021798	25	0.007548	0.007548	0.00000032
1.22	0.74	0.952579	0.968406	1	0.006778	0.006778	0.00000037

The comparison showed the difference between the 2 pair of values being very small (less than 0.01%) hence showing that ANNs can be used for the online prediction of VCPI values for the Kenya Power system.

From the foregoing results, an extension was made to use CART decision trees in predicting the voltage magnitude at the load buses as discussed next.

4.5 Developing of CART Algorithm using the IEEE 30 – Bus System

Since a previous study [14] had identified buses 26,29 and 30 as the weakest bus in the system, CART trees were plotted using the algorithm described in section 3.3.2. The resulting decision tree for bus 26 plotted using 3000 minimum observations for a node to be split is shown in Figure 4.6 below;

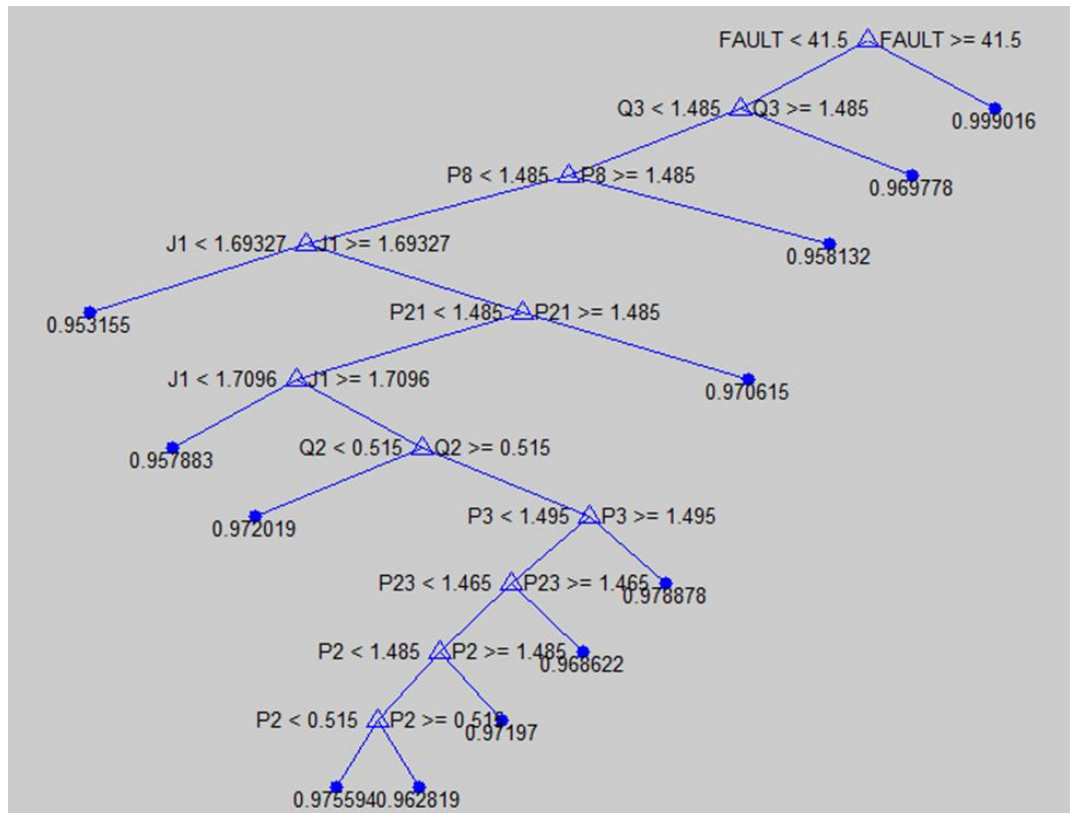


Figure 4.6: CART Tree (3000 Minimum Observations) Bus 26 – IEEE 30 Bus System

From the algorithm, the iteration using the base case (without a line contingency) is stored as the 42nd load-contingency configuration. From Figure 4.6, the CART tree shows the FAULT as the most significant variable affecting the voltage magnitude. Without any line fault (FAULT = 42), the voltage magnitude at bus 26 is at 0.999 p.u. but varies in the presence of any line fault in the system, depending on the other variables which form the other nodes in the decision tree. The CART tree makes it possible to see which variables affect the voltage magnitude at bus 26 the most. From Figure 4.6, the 5 most significant variables to the voltage magnitude at bus 26 are the

fault, Q_3 – reactive power demand at bus 3, P_8 – real power demand at bus 3 J_1 – change in real power demand at bus 1 with change in the power factor at bus 1 and P_{21} – real power demand at bus 21.

The presence of the fault is expected to affect power flows within the system and thus it has the greatest influence on the voltage magnitude on many buses, including bus 26.

Bus 3 is a relatively small bus with a load of $(2.4+j1.2)$ MVA. Its connection to the slack bus and bus 4 both of which have voltage magnitudes greater than 1p.u. is what makes the reactive demand at bus 3 to be an influence on the voltage magnitude at bus 26.

Bus 8 has a comparatively large highly inductive load $(30+j30)$ MVA which is 11% of total real power demand and 24% of the total reactive power demand in the system. It has the lowest pf in the system 0.71 and also has reactive compensation hence the real power demand at this bus affects the voltage magnitude at bus 26 and other buses.

J_1 is an indicator of the sensitivity of the power demand at bus 26 to the power factor and also has an influence on the voltage magnitude as expected.

Bus 21 is a comparatively large load $(17.5+j11.2)$ MVA. In addition, it is only connected radially to bus 10 which has reactive compensation. This means that while its reactive load may be compensated by the static compensation, the real power demand will affect power flows within the rest of the system including bus 26.

In order to reduce the size of the CART decision tree, the minimum number of observations required for a terminal node were increased to 4000 giving the CART decision tree in Figure 4.7 which was pruned by two levels to give the minimum tree in Figure 4.8;

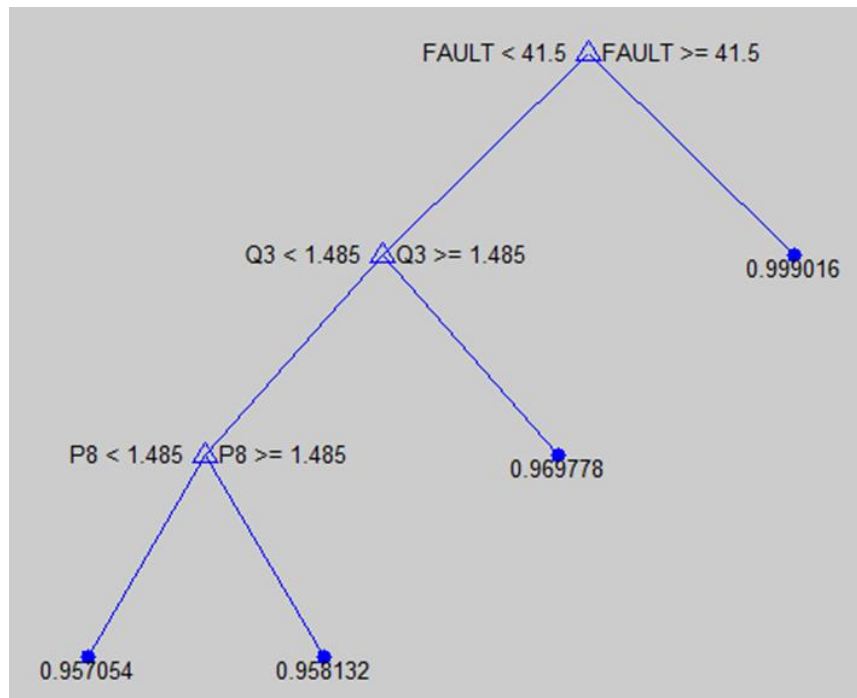


Figure 4.7: CART Tree (4000 Minimum Observations) Bus 26 – IEEE 30 Bus System

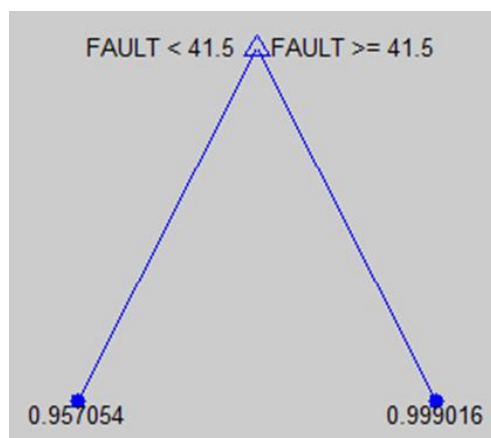


Figure 4.8: CART Tree (Pruned 2 levels) Bus 26 – IEEE 30 Bus System

4.6 CART Based Analysis - Kenya Power System

The algorithm described in section 3.5 was applied to the Kenya Power System. In addition, taking from the results in section 4.4 for the IEEE 30 – Bus System, a minimum number of observations for node splitting was selected at 3500 to give a balance between capturing the most influential variables without going into too much

detail in the CART decision tree. Buses 10 and 30 were the main focus since they had earlier [14] been identified as the weak buses. The CART trees resulting are shown below;

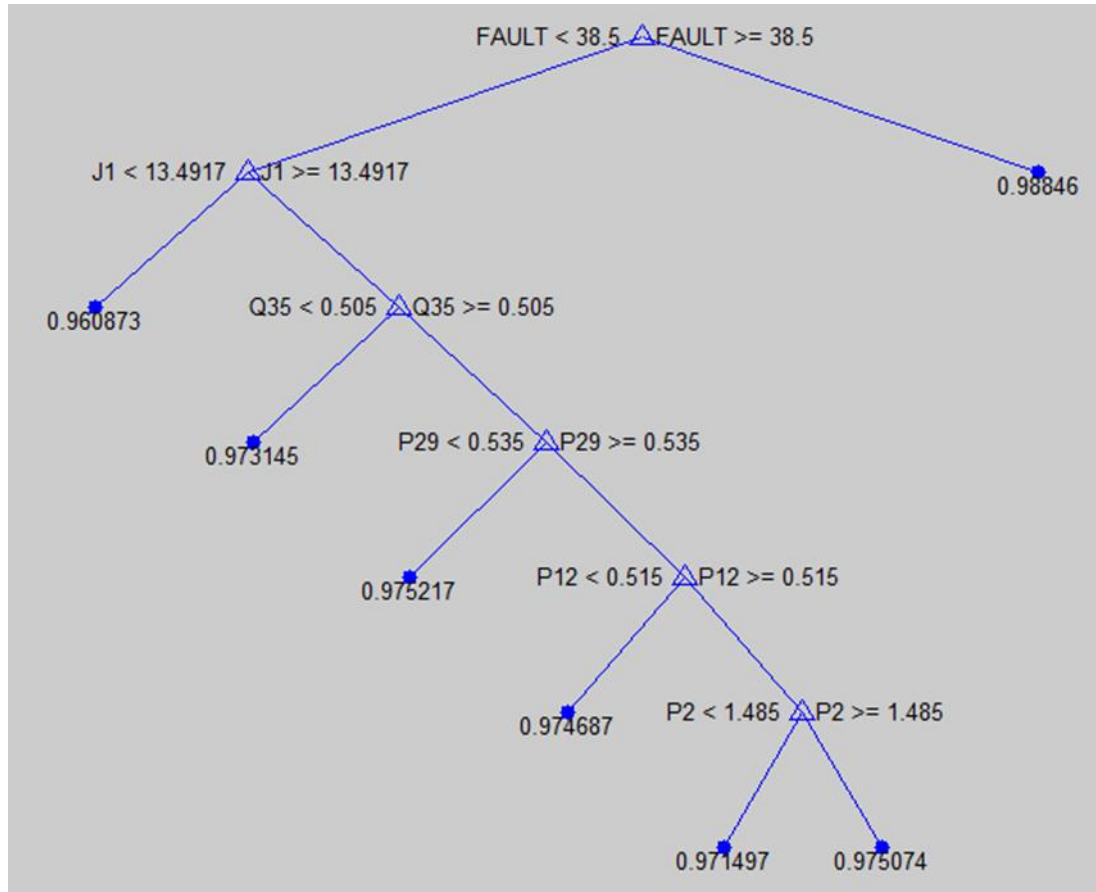


Figure 4.9: CART Tree (3500 Minimum Observations) Bus 10 – Kenya Power System

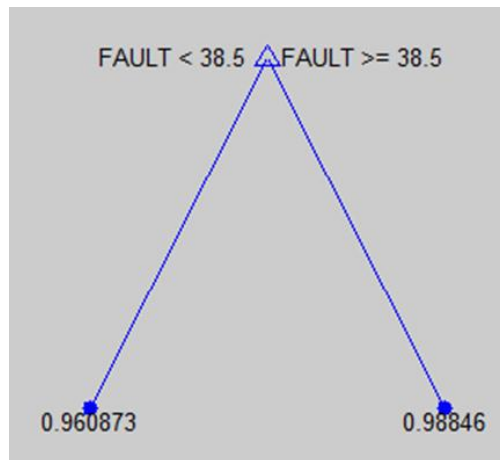


Figure 4.10: CART Tree (Level 2 Pruned) Bus 10 – Kenya Power System

From Figure 4.9, excluding the single – line contingency, the 5 most influential variables influencing the voltage at bus 10 are the fault, J_1 , Q_{35} , P_{29} and P_{12} .

J_1 represents the sensitivity of the real power at bus 10 to the power factor which as expected would influence the voltage magnitude at bus 10.

Bus 35 is physically and electrically distant from bus 10. It's intriguing that its reactive power demand would affect the voltage magnitude of bus 10 so far away. Also interesting is the range of the split at the node due to the reactive power at bus 35, 0.505p.u. Bus 35 has a relatively small load (8.1+j1.3) MVA. This means that the threshold above which it influences the voltage at bus 10 is also very low. Both bus 10 and bus 35 are terminal buses connected radially quite far from the main generators. The distance that reactive power has to travel from the generators and compensators to the buses is hence quite long meaning that when reactive power demand is high at one end, it reduces the amount of reactive power available at the opposite end and thus affects the voltage magnitudes.

Bus 29 is also electrically distant from bus 10 and on the opposite end of the power system. It therefore has a similar effect as bus 35 with a similarly low split in the real power demand 0.035p.u. that affects voltage at bus 10.

Bus 12 on the other hand is close to bus 10. However, it is connected to bus14 which is a generator bus. Since the generator at bus 14 is the closes to bus 10, then the real

power demand at bus 12 affects the real power available to bus 10 and thus affects its voltage.

Figure 4.10 shows the effect of any line contingency on the voltage at bus 10. As expected, it is low when there is a fault (0.961p.u.) and slightly higher (0.988p.u.) when there is no fault.

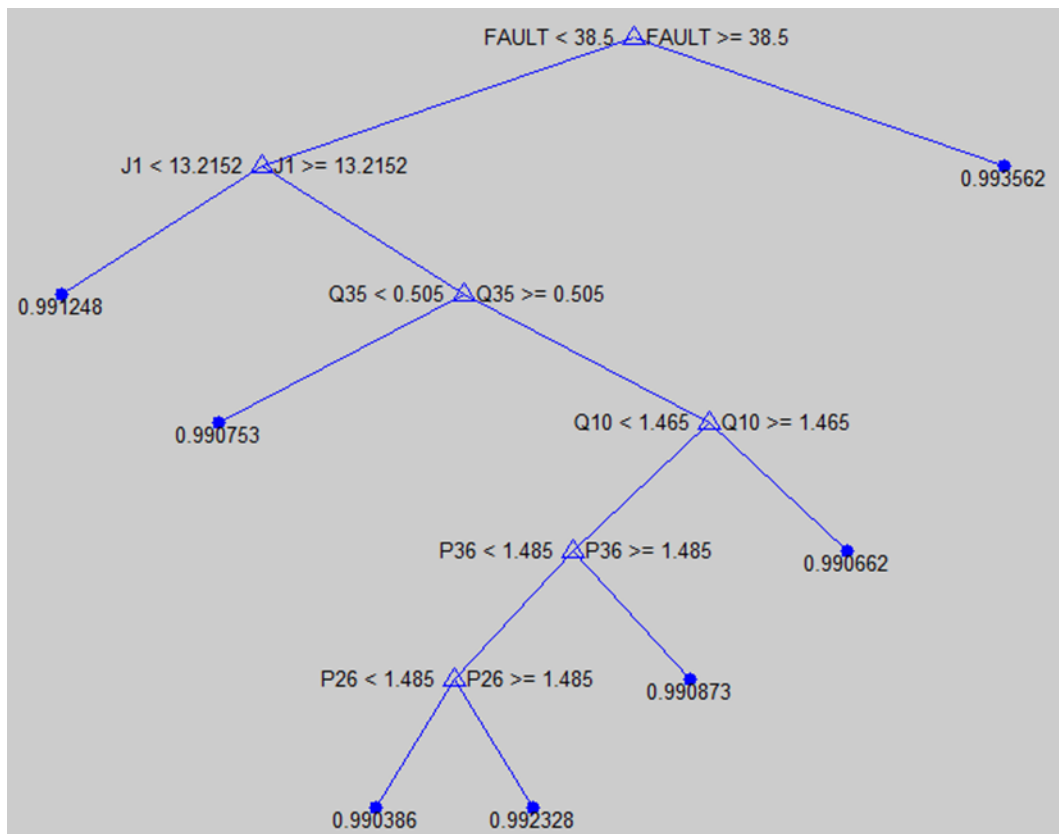


Figure 4.11: CART Tree (3500 Minimum Observations) Bus 30 – Kenya Power System

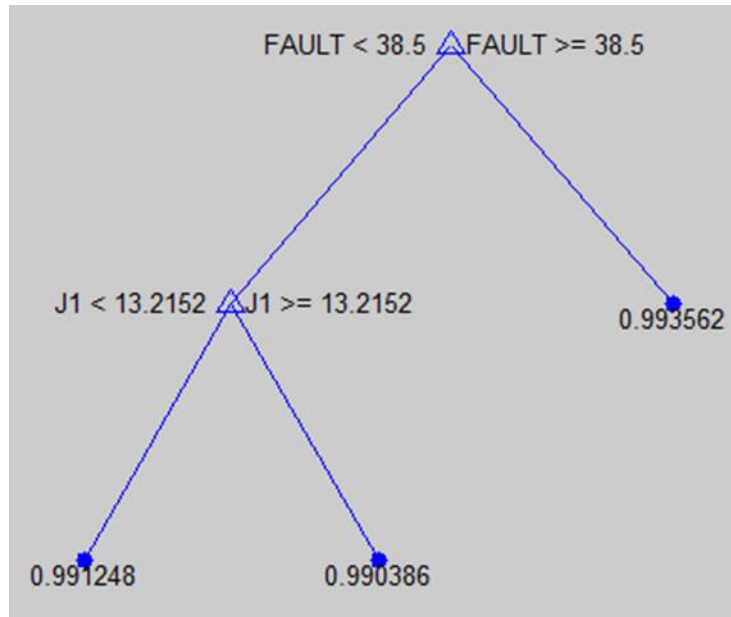


Figure 4.12: CART Tree (Level 1 Pruned) Bus 30 – Kenya Power System

From Figure 4.11 for the CART tree for bus 30, the effect of buses at the extremes of the system, bus 10 and bus 35, is reflected with the reactive power demands at the two buses having a considerable effect on the voltage magnitude at bus 30. Also, the pruned tree for bus 30 as shown in Figure 4.12 shows that the fault and the sensitivity of the real power demand at bus 30 to the power factor have a similar weight in their effect on the voltage at bus 30.

The CART trees for the other load buses showed a similar trend as those for the weak buses 10 and 30 as given in the appendix. For all the buses, the fault has the highest effect on their bus voltages and the absence of a fault has most of the buses having a voltage magnitude of between 0.98p.u. and 1.01p.u. In addition, the most common variables affecting most of the buses are $Q_5, P_{25}, P_{29}, P_{12}, P_3, P_{13}, P_{11}$ and Q_{35} . Bus 3 (22+j11)MVA and Bus 5 (15.9+j6.3)MVA are the largest loads in the western side of the system and it would thus so follow that power demand at these buses would have a larger effect on the voltage magnitude at other buses in the system. Bus 25 (1.8+j0)MVA, bus 29 (4.3+j1)MVA and bus 35 (8.5+j1.3)MVA are relatively small loads but are located physically far away from the large generators within the system. This means that their electrical distance is also larger due to the line impedance required to cover the long physical distances. The load demand at

these buses therefore tends to affect other buses' voltage magnitudes. Similarly, due to their small magnitudes, their effect when measured in p.u. would appear larger. Bus 11 $(16+j4.7)$ MVA , bus 12 $(7.5+j4.8)$ MVA, and bus 13 $(53+j26)$ MVA are relatively large loads located near the central region of the country and also near the major generators. It follows that their power demand would have a pronounced effect of other buses given that power can flow much easily to them compared to distant buses within the system.

4.7 Conclusion

In this chapter, the results of the research are presented. The VCPI verification algorithm as tested on the IEEE 9 – Bus system are presented as compared to those from literature. The comparison of the values of the VCPI index for the IEEE 30 – Bus system using the conventional load flow calculation with those predicted using an ANN showed the capacity of using an ANN as a predictor instead of using the conventional load flow calculation which takes a longer period to calculate. The extension of the prediction to using CART trees for dynamic voltage stability analysis as tested on the IEEE 30 – Bus system before being applied on the Kenya Power system showed the capacity of CART trees to predict the likely value of the voltage magnitude at the weak buses within the systems based on the power demands at other buses within the 2 systems.

CHAPTER FIVE

CONCLUSIONS AND RECOMMENDATIONS

From the results, the research was successfully carried out with decision trees being constructed for all the load buses within the system. Specifically, the following stood out;

The results for the VCPI from the IEEE 9 – bus were able to match those from previous study and this validated the algorithm used in calculation of the VCPI. The same algorithm was extended to the IEEE 30 – bus and the Kenya Power System and used in the calculation of the VCPI indices for the various buses for steady load increments as well as randomised loading. In addition, the use of ANNs to predict the VCPI gave results which closely matched those from the use of the conventional load flow method. This indicated that the use of artificial intelligence could be extended to calculate the VCPI without necessarily using the load flow calculation. Also, the validation of the VCPI meant that the variables used in its calculation could be used independent of the VCPI as is the case in the application of CART decision trees.

Using the methodology developed, the main variables used in calculating the VCPI were extracted and used in the construction of the CART decision trees for the IEEE – 30 Bus and the Kenya Power System as required in the main objective of the thesis. The CART decision trees showed the following regarding the dynamic voltage of the load buses in the system;

- i. The absence or presence of a line fault has the greatest effect on all load buses within the system, as predicted in all the CART trees for the IEEE systems and the Kenya Power System
- ii. The Jacobian sub – matrix J_1 for all buses has the greatest effect on the voltage at the load bus. This was expected since the J_1 component of the Jacobian matrix relates to sensitivity of the real power to changes in the power factor.

- iii. The analysis of the weak buses using the CART decision trees indicated that different buses are affected by the real and reactive power demand at various other buses within the system. The use of the CART decision tree shows the power demands that affect the voltage magnitude at a particular bus and also in the order of the magnitude of their effect on the voltage magnitude of the bus in question.
- iv. The CART decision tree method can relate different buses that are located physically and electrically apart. Buses located physically and electrically further away from the main system generators were seen to have an effect on the voltage magnitude of load buses. This was an unexpected phenomenon and shows that the CART decision tree can find relationships by data mining of information related to buses that are not easily detected otherwise.

In order to mitigate dynamic voltage instability, the following measures are suggested;

- i. The system operator should focus on the main buses whose active and reactive loads are seen to affect the voltage magnitude at other distant or weak load buses e.g. buses 25, 29 and 35 should always have their loads being monitored as increases in these buses' loads affects the voltage at multiple buses within the system.
- ii. In case of reactive power support, the reactive power supply should also be placed at these major buses in order to meet their load demands and reduce their effect on other distant load buses.
- iii. In case of impending voltage collapse, as a last resort, load shedding can be carried out in order to maintain voltage stability. The 3 main buses, 25, 29 and 35, should be the first to be load shed in order to maintain voltage stability of the rest of the system by reducing load demand at these main buses.

Further research areas recommended from this work could include;

- i. An analysis of the correlation between the buses whose real or reactive power affects many buses and the impact which support measures like distributed

generation and reactive power support would have on other buses if the support was located at these buses.

- ii. The use of Fuzzy Logic or a similar artificial intelligence method in developing an online SCADA based system for predictive voltage protection.

REFERENCES

- [1] P. Kundur , “*Power System Stability and Control* “, NY, USA : McGraw-Hill Inc ; 1994.
- [2] IEEE-PES Power Systems Stability Subcommittee, “*Voltage Stability Assessment: Concepts, Practices and Tools*”, Subcommittee Special Publication, IEEE Catalog Number SP101PSS, August 2002.
- [3] R. Silva , “Discussion on Voltage Stability of Transmission Augmentations into Auckland”, (Revision 1) ,Auckland, New Zealand, January 2007.
- [4] CIGRE SC38-WG02 Report, “*State of the Art in Non-Classical Means to Improve Power System Stability*”, Electra, No. 118, May 1988.
- [5] L. Cai, and I. Erlich, “Power System Static Voltage Stability Analysis Considering all Active and Reactive Power Controls - Singular Value Approach”, in *IEEE Power Tech – IEEE Lausanne* ,July 2007.
- [6] L. Cai, and I. Erlich, “Dynamic Voltage Stability Analysis In Multi-Machine Power Systems”, in IEEE Power Tech, in *IEEE Power Tech – IEEE Lausanne* ,July 2007.
- [7] C.A. Canizares: “Basic theoretical concept, Voltage stability indices”, in IEEE Power Engineering Society, August 2004.
- [8] V. Balamourougan: “Technique for Online Prediction of Voltage Collapse”, in *IEEE Proceedings on Generation, Transmission and Distribution*, Vol.151, No. 4, July 2004, pp. 453-460.
- [9] G. M. Haung and N. Kumar, “Detection of Dynamic Voltage Collapse”, in *IEEE Power Engineering Society Summer Meeting*, , 2002.
- [10] S. Meshram and O. Sahu, “Application of ANN in Economic Generation Scheduling in IEEE 6 – Bus System”, *International Journal of Engineering Science and Technology (IJEST)*, Vol. 3 No. 3, March 2011.
- [11] K. Sun et al, “An Online Dynamic Security Assessment Scheme Using Phasor Measurements and Decision Trees”, *IEEE Transactions On Power Systems*, Vol. 22, No. 4, November 2007, pp 1935.
- [12] Y. Yohannes and J. Hoddinott, “Classification and Regression Trees: An Introduction”, International Food Policy Research Institute, Technical Guide No. 3, March 1999.
- [13] R. A. Alammari, “Fuzzy System Applications for Identification of Weak buses in Power Systems”, *The Arabian Journal for Science and Engineering, King Fahd University*, Vol. 27, October 2002, pp. 165-178.
- [14] C. Muriithi and S. Njoroge , “Voltage Stability Analysis Using CP_ANN and Optimized Capacitor Bank Placement”, in *JKUAT SRI Conference*, June 2010.

- [15] L. Cai, and I. Erlich, "Dynamic Voltage Stability Analysis In Multi-Machine Power Systems", in *IEEE Power Tech – IEEE Lausanne*, July 2007.
- [16] K. Ioannis and O. Konstadinos, "An Analytical approach for Dynamic Voltage Stability Analysis in Power Systems", *Proceedings of the 5th WSEAS International Conference on Applications of Electrical Engineering*, Prague, Czech Republic, March 2006 (pp36-38).
- [17] B. N. Soni, "Bifurcation Analysis for Voltage Stability of Power System", in *National Conference on Recent Trends in Engineering & Technology*, May 2011
- [18] L. Cai et al, "Power System Dynamic Voltage Stability Analysis for Integration of Large Scale Wind Parks", in *9th International Workshop on Large-Scale Integration of Wind Power into Power Systems as well as on Transmission Networks for Offshore Wind Power Plants*, Quebec City, Quebec, Canada, October, 2010
- [19] E. S. Karapidakis and N. D. Hatziaargyriou, "Online Preventive Dynamic Security of Isolated Power Systems Using Decision Trees", *IEEE Transactions On Power Systems*, Vol. 17, No. 2, May 2002 pp. 297 – 304
- [20] C. Subramani et al, "Voltage Stability Based Collapse Prediction and Weak Cluster Identification", *International Journal of Electrical and Power Engineering* Vol. 3 No. 2, 2009, pp.124-128
- [21] N. Izzri et al, "Fast Prediction of Power Transfer Stability Index Based on Radial Basis Function Neural Network", *International Journal of the Physical Sciences* Vol. 6(35), 23 December 2011, pp. 7978 - 7984,
- [22] I. Kumaraswamy et al, "An Optimal Power Flow (OPF) Method with Improved Voltage Stability Analysis", in *Proceedings of the World Congress on Engineering 2012 Vol II WCE*, London, U.K , July 2012,.
- [23] G. Balamurugan and P. Aravindhababu , "ANN Based Online Estimation of Voltage Collapse Proximity Indicator", *International Journal of Engineering Science and Technology* Vol. 2(7), 2010, pp. 2869-2875
- [24] C. Reis and F. Barbosa , "A Comparison of Voltage Stability Indices", in *IEEE MELECON 2006*, May 2006, pp. 1007-1010.
- [25] I. Musirin and T. A. Rahman, "Novel Fast Voltage Stability Index (FVSI) for Voltage Stability Analysis in Power Transmission System", in *Research and Development Student Conference on SCOREd*, 2002, pp. 265-268.
- [26] M. Moghavvemi and F. Omar, "Technique for Contingency Monitoring and Voltage Collapse Prediction" in *IEEE Proceedings on Generation, Transmission and Distribution*, Vol. 145, N6, 1998, pp. 634-640

- [27] A. Mohamed et al, "A Static Voltage Collapse Indicator using Line Stability Factors" *Journal of Industrial Technology*, Vol.7, No.1, 1989, pp. 73-85
- [28] O. Maimon and L. Rokach , *Data Mining and Discovery Handbook* , Springer Science and Business Media, Inc. NY, USA, 2005, pp. 165-174.
- [29] T. Pang-Ning et al, *Introduction to Data Mining*, Pearson Educational Publishers, NY, USA, 2005, pp.150-160.
- [30] Quinlan, J.R., *Induction of Decision Trees*, Kluwer Academic Publishers Hingham, MA, USA, 1986, pp81-106.
- [31] Quinlan, J. R., *C4.5: Programs for Machine Learning*, Morgan Kaufmann Publishers, Los Altos, USA, 1993.
- [32] O. Maimon and L. Rokach, *Data Mining and Knowledge Discovery Handbook*, Springer US, NY, USA, 2010.
- [33] T. Yun et al., "Regional Voltage Stability Prediction Based on Decision Tree Algorithm", in *IEEE Intelligent Transportation Conference, Big Data and Smart City (ICITBS)*, 2015, pp588-591.
- [34] M. Cernak, "A Comparison of Decision Tree Classifiers for Automatic Diagnosis of Speech Recognition Errors, Text, Speech and Dialogue", in *13th International Conference, Computing and Informatics*, Vol 29, 2010, pp 489-501.
- [35] E. Leonidaki and N. Hatziargyriou, "Investigation of Decision Tree(s) Parameters for Power System Voltage Stability Enhancement", *SETN 2006*, Springer-Verlag Berlin Heidelberg 2006, pp 181-191.

APPENDIX

Appendix A1: IEEE 9 - Bus System

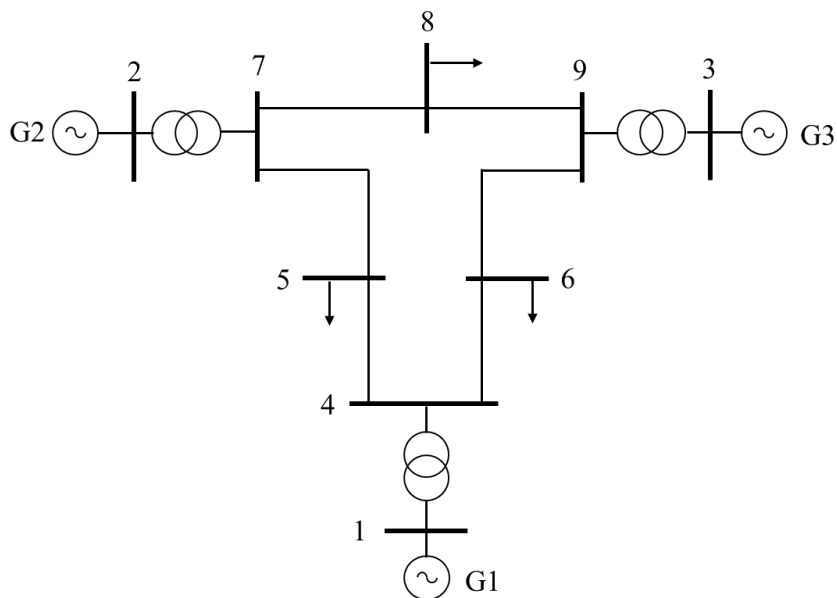


Figure A1: IEEE 9 – Bus System

Table A.1: IEEE 9 – Bus System Bus Data

MVA_{base} = 100MVA				Load		Generation				
Bus No	Bus Code	 V 	δ	MW	Mvar	MW	Mvar	Qmin	Qmax	Injected
1	1	1	0	0	0	247.5	0	0	0	0
2	2	1	0	0	0	163.2	0	0	101.14	0
3	2	1	0	0	0	108.8	0	0	67.428	0
4	0	1	0	0	0	0	0	0	0	0
5	0	1	0	125	50	0	0	0	0	0
6	0	1	0	90	30	0	0	0	0	0
7	0	1	0	0	0	0	0	0	0	0
8	0	1	0	100	35	0	0	0	0	0
9	0	1	0	0	0	0	0	0	0	0

Table A.2: IEEE 9 – Bus System Line Data

Bus No	Bus No	R	X	1/2B	Tranformer tap setting
n_l	n_r	pu	pu	pu	
1	4	0	0.0576	0	1
2	7	0	0.0625	0	1
3	9	0	0.0586	0	1
4	5	0.01	0.085	0.088	1
4	6	0.017	0.092	0.079	1
5	7	0.032	0.161	0.153	1
6	9	0.039	0.17	0.179	1
7	8	0.0085	0.072	0.0745	1
8	9	0.0119	0.1008	0.1045	1

Appendix A2: IEEE 30 - Bus System

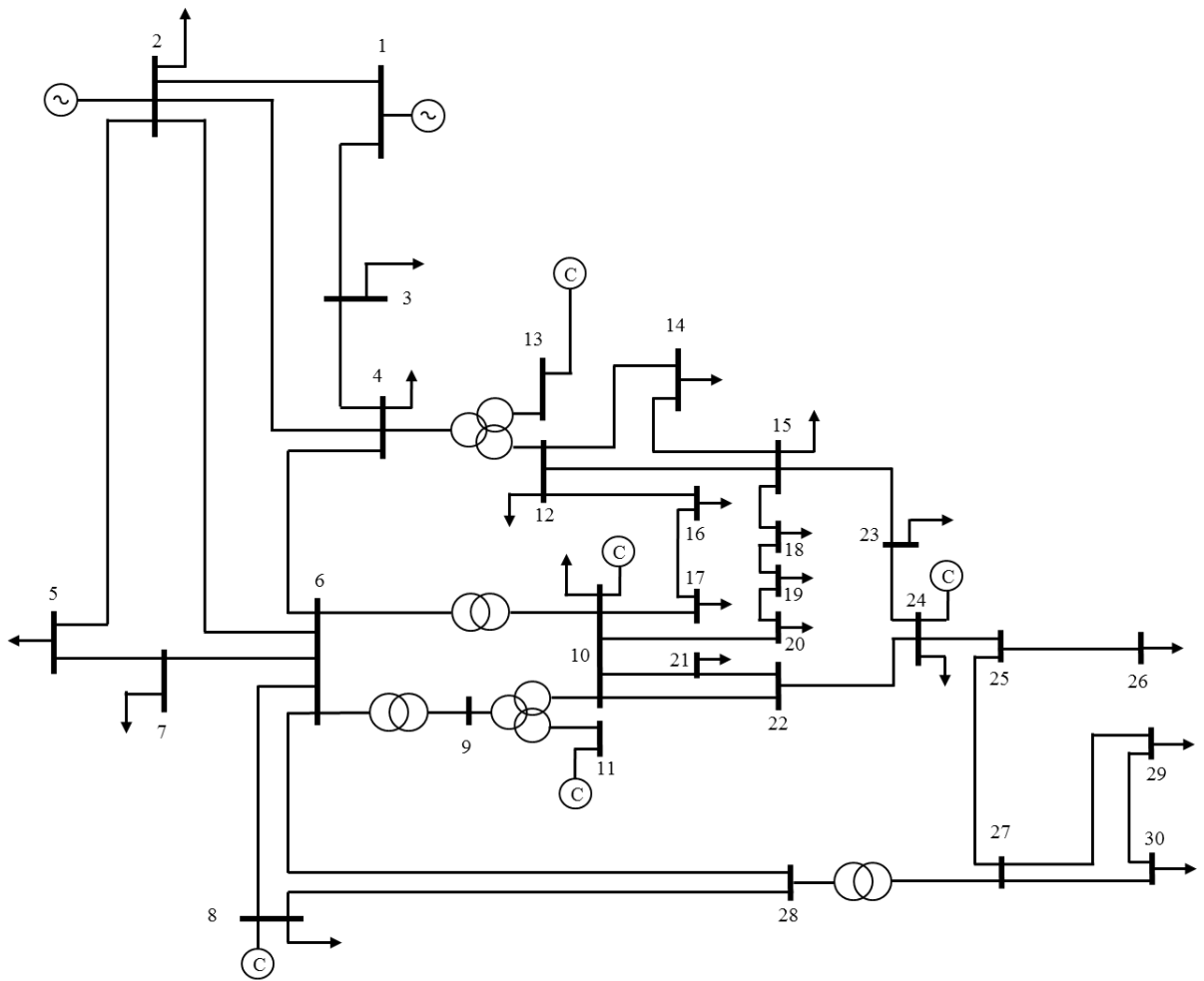


Figure A2: IEEE 30 – Bus System

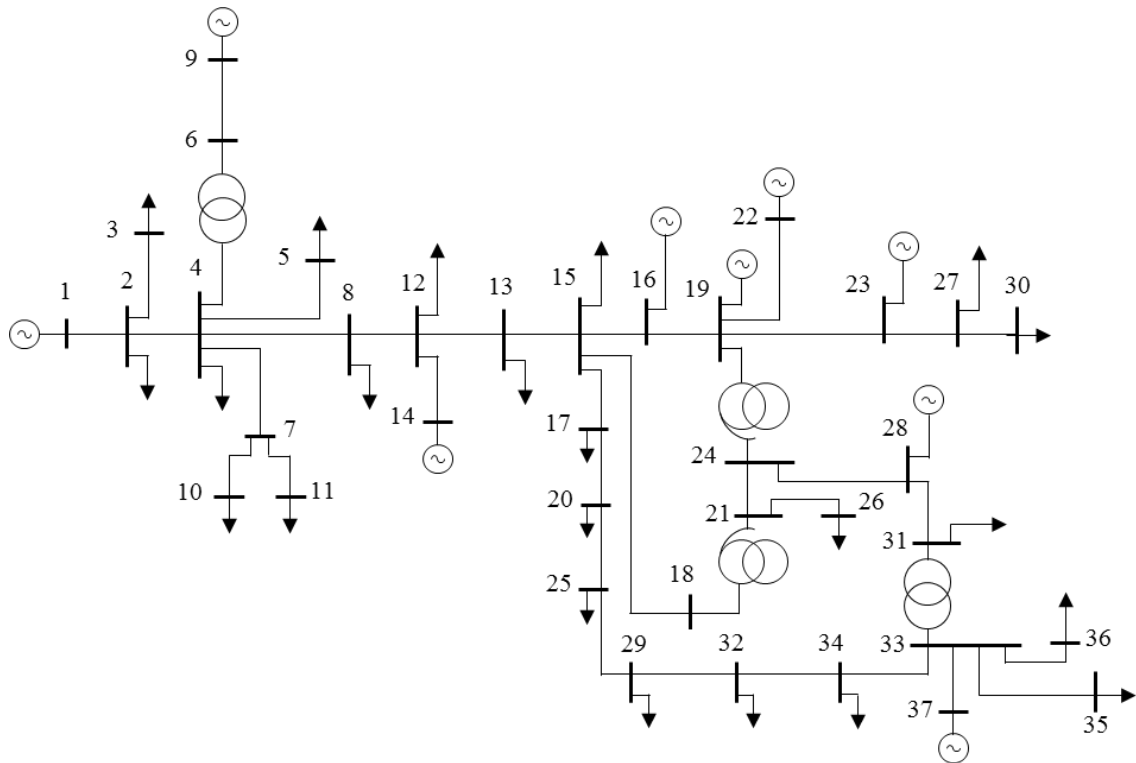
Table A.3: IEEE 30 – Bus System Bus Data

MVA_{base} = 100MVA				Load		Generation				
Bus No	Bus Code	 V 	δ	MW	Mvar	MW	Mvar	Qmin	Qmax	Injected
1	1	1.06	0	0	0	0	0	0	0	0
2	2	1.043	0	21.7	12.7	40	0	-40	50	0
3	0	1	0	2.4	1.2	0	0	0	0	0
4	0	1.06	0	7.6	1.6	0	0	0	0	0
5	2	1	0	94.2	19	0	0	-40	40	0
6	0	1	0	0	0	0	0	0	0	0
7	0	1	0	22.8	10.9	0	0	0	0	0
8	2	1.01	0	30	30	0	0	-30	40	0
9	0	1	0	0	0	0	0	0	0	0
10	0	1	0	5.8	2	0	0	-6	24	19
11	2	1.082	0	0	0	0	0	0	0	0
12	0	1	0	11.2	7.5	0	0	0	0	0
13	2	1.071	0	0	0	0	0	-6	24	0
14	0	1	0	6.2	1.6	0	0	0	0	0
15	0	1	0	8.2	2.5	0	0	0	0	0
16	0	1	0	3.5	1.8	0	0	0	0	0
17	0	1	0	9	5.8	0	0	0	0	0
18	0	1	0	3.2	0.9	0	0	0	0	0
19	0	1	0	9.5	3.4	0	0	0	0	0
20	0	1	0	2.2	0.7	0	0	0	0	0
21	0	1	0	17.5	11.2	0	0	0	0	0
22	0	1	0	0	0	0	0	0	0	0
23	0	1	0	3.2	1.6	0	0	0	0	0
24	0	1	0	8.7	6.7	0	0	0	0	4.3
25	0	1	0	0	0	0	0	0	0	0
26	0	1	0	3.5	2.3	0	0	0	0	0
27	0	1	0	0	0	0	0	0	0	0
28	0	1	0	0	0	0	0	0	0	0
29	0	1	0	2.4	0.9	0	0	0	0	0
30	0	1	0	10.6	1.9	0	0	0	0	0

Table A.4: IEEE 30 – Bus System Line Data

Bus No	Bus No	R	X	1/2B	Tranformer tap setting
n_l	n_r	pu	pu	pu	
1	3	0.0452	0.1852	0.0204	1
2	4	0.057	0.1737	0.0184	1
3	4	0.0132	0.0379	0.0042	1
2	5	0.0472	0.1983	0.0209	1
2	6	0.0581	0.1763	0.0187	1
4	6	0.0119	0.0414	0.0045	1
5	7	0.046	0.116	0.0102	1
6	7	0.0267	0.082	0.0085	1
6	8	0.012	0.042	0.0045	1
6	9	0	0.208	0	0.978
6	10	0	0.556	0	0.969
9	11	0	0.208	0	1
9	10	0	0.11	0	1
4	12	0	0.256	0	0.932
12	13	0	0.14	0	1
12	14	0.1231	0.2559	0	1
12	15	0.0662	0.1304	0	1
12	16	0.0945	0.1987	0	1
14	15	0.221	0.1997	0	1
16	17	0.0824	0.1923	0	1
15	18	0.1073	0.2185	0	1
18	19	0.0639	0.1292	0	1
19	20	0.034	0.068	0	1
10	20	0.0936	0.209	0	1
10	17	0.0324	0.0845	0	1
10	21	0.0348	0.0749	0	1
10	22	0.0727	0.1499	0	1
21	22	0.0116	0.0236	0	1
15	23	0.1	0.202	0	1
22	24	0.115	0.179	0	1
23	24	0.132	0.27	0	1
24	25	0.1885	0.3292	0	1
25	26	0.2544	0.38	0	1
25	27	0.1093	0.2087	0	1
28	27	0	0.396	0	0.968
27	29	0.2198	0.4153	0	1
27	30	0.3202	0.6027	0	1
29	30	0.2399	0.4533	0	1
8	28	0.0636	0.2	0.0214	1
6	28	0.0169	0.0599	0.065	1

Appendix A3: Kenya Power System (37-Bus Model)



Bus No	Location	Bus No	Location	Bus No	Location	Bus No	Location
1	Tororo	11	Chemosit	21	Dandora	31	Rabai
2	Musaga	12	Naivasha	22	Gitaru	32	Mangu
3	Webuye	13	Ruaraka	23	Masinga	33	Rabai
4	Lessos	14	OlKaria	24	Kamburu	34	Mariakani
5	Eldoret	15	Juja	25	Mtito Andei	35	Kilifi
6	Lessos	16	Kin daruma	26	Embakasi	36	Bamburi
7	Muhoroni	17	Sultan Hamud	27	Kiganjo	37	Kipevu
8	Lanet	18	Dandora	28	Kiambere		
9	Turkwell	19	Kamburu	29	Voi		
10	Kisumu	20	Kiboko	30	Nanyuki		

Figure A3: Kenya Power System

Table A.5: Kenya Power System Bus Data

MVA_base = 100MVA				Load		Generation				
Bus No	Bus Code	Vmag	Angle	MW	Mvar	MW	Mvar	Qmin	Qmax	Injected
1	1	1	0	0	0	0	0	0	0	0
2	0	1	0	13	6	0	0	0	0	0
3	0	1	0	22	11	0	0	0	0	0
4	0	1	0	9.2	4	0	0	0	0	0
5	0	1	0	15.9	6.3	0	0	0	0	0
6	0	1	0	0	0	0	0	0	0	0
7	0	1	0	0	0	0	0	0	0	0
8	0	1	0	33.5	21	6 0	0	0	0	0
9	2	1	0	0	0	106	65.72	0	0	0
10	0	1	0	18	5.3	0	0	0	0	0
11	0	1	0	16	4.7	0	0	0	0	0
12	0	1	0	7.5	4.8	0	0	0	0	0
13	0	1	0	53	26	0	0	0	0	0
14	2	1	0	0	0	27.5	17.05	0	0	0
15	0	1	0	95	46	0	0	0	0	0
16	2	1	0	0	0	40	24.8	0	0	0
17	0	1	0	0.8	0	0	0	0	0	0
18	0	1	0	0	0	0	0	0	0	0
19	2	1	0	0	0	225	139.5	0	0	0
20	0	1	0	0.2	0	0	0	0	0	0
21	0	1	0	0	0	0	0	0	0	0
22	2	1	0	0	0	94.2	58.4	0	0	0
23	2	1	0	0	0	0	0	0	0	0
24	0	1	0	0	0	0	0	0	0	0
25	0	1	0	1.8	0	0	0	0	0	0
26	0	1	0	84	54	0	0	0	0	0
27	0	1	0	10	4.8	0	0	0	0	0
28	2	1	0	0	0	44	27.28	0	0	0
29	0	1	0	4.3	1	0	0	0	0	0
30	0	1	0	12	5.8	0	0	0	0	0
31	0	1	0	0	0	0	0	0	0	0
32	0	1	0	0.9	0	0	0	0	0	0
33	0	1	0	15.5	14	0	0	0	0	0
34	0	1	0	6.8	3.3	0	0	0	0	0
35	0	1	0	8.1	1.3	0	0	0	0	0
36	0	1	0	13.8	6.7	0	0	0	0	0
37	2	1	0	79.8	38.7	63	39.06	0	0	0

Table A.6: Kenya Power System Line Data

n_l	n_r	R	X	1/2B	Tran. Tap.
24	21	0.001663	0.010124	0.01655	1
24	28	0.001529	0.00624	0.01111	1
28	31	0.019153	0.078326	0.13948	1
6	9	0.009483	0.038802	0.69115	1
21	26	0.000196	0.001209	0.00192	1
1	2	0.024277	0.017593	0.00143	1
2	3	0.012397	0.008988	0.00073	1
2	4	0.022498	0.016374	0.00134	1
4	5	0.022096	0.016074	0.00131	1
4	7	0.039027	0.028306	0.0023	1
7	11	0.02112	0.015331	0.00225	1
7	10	0.033402	0.024256	0.00197	1
4	8	0.042958	0.031612	0.00256	1
8	12	0.023072	0.016725	0.00136	1
12	14	0.023072	0.016725	0.00136	1
12	13	0.00551	0.011839	0.00092	1
13	15	0.001435	0.00125	0.0001	1
19	23	0.000517	0.000372	0.00003	1
15	16	0.070535	0.060393	0.00477	1
16	19	0.010904	0.009339	0.00074	1
23	27	0.002296	0.001952	0.00002	1
22	19	0.06095	0.044174	0.00358	1
27	30	0.035468	0.025702	0.00209	1
15	17	0.074093	0.06343	0.00501	1
17	20	0.025482	0.021818	0.00171	1
20	25	0.050964	0.043636	0.00385	1
25	29	0.053375	0.045682	0.00361	1
29	32	0.016586	0.018347	0.00112	1
32	34	0.050964	0.043636	0.00345	1
33	34	0.014233	0.010537	0.00084	1
33	36	0.011708	0.008492	0.00069	1
33	37	0.023072	0.016725	0.00136	1
33	35	0.031279	0.022665	0.00185	1
15	18	0.000459	0.000103	0.00008	1
6	4	0.0021	0.0706	0	0.9
19	24	0.0021	0.0706	0	0.9
21	18	0.0021	0.0706	0	0.9
31	33	0.0021	0.0706	0	0.9

Appendix A4: ANN vs Load Flow Calculation for VCPI Calculation

Table A.7: Comparison of VCPI Values Using Load Flow Calculations and ANNs for IEEE 14 – Bus System [25]

Test Case	Input (all quantities in per unit)				Method	Output / VCPI		
	P_L^{14}	Q_L^{14}	P_{NET}	Q_{NET}		L_0^{14}	L_1^{14}	L_2^{14}
1	0.1300	0.0700	2.7000	1.6000	CA	0.1224	0.2039	0.1339
					PA	0.1228	0.2034	0.1347
2	0.1500	0.0900	1.8000	1.3500	CA	0.0911	0.1408	0.0941
					PA	0.0914	0.1409	0.0947
3	0.1800	0.0800	2.1000	1.0100	CA	0.0893	0.1359	0.0904
					PA	0.0897	0.1354	0.0918
4	0.2200	0.1300	2.1000	1.5800	CA	0.1327	0.2102	0.1442
					PA	0.1329	0.2100	0.1440
5	0.3500	0.1750	3.6000	1.2000	CA	0.2360	0.4381	0.2685
					PA	0.2360	0.4381	0.2685

Appendix A5: Selected CART Decision Trees For Kenya Power System Load Buses

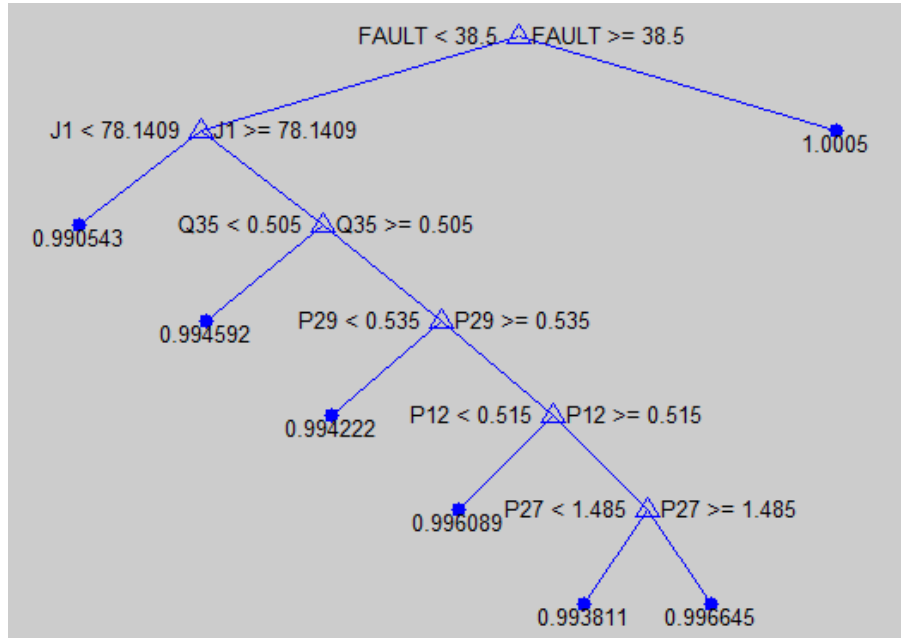


Figure A5.1: CART Tree (3500 Minimum Observations) Bus 2 – Kenya Power System

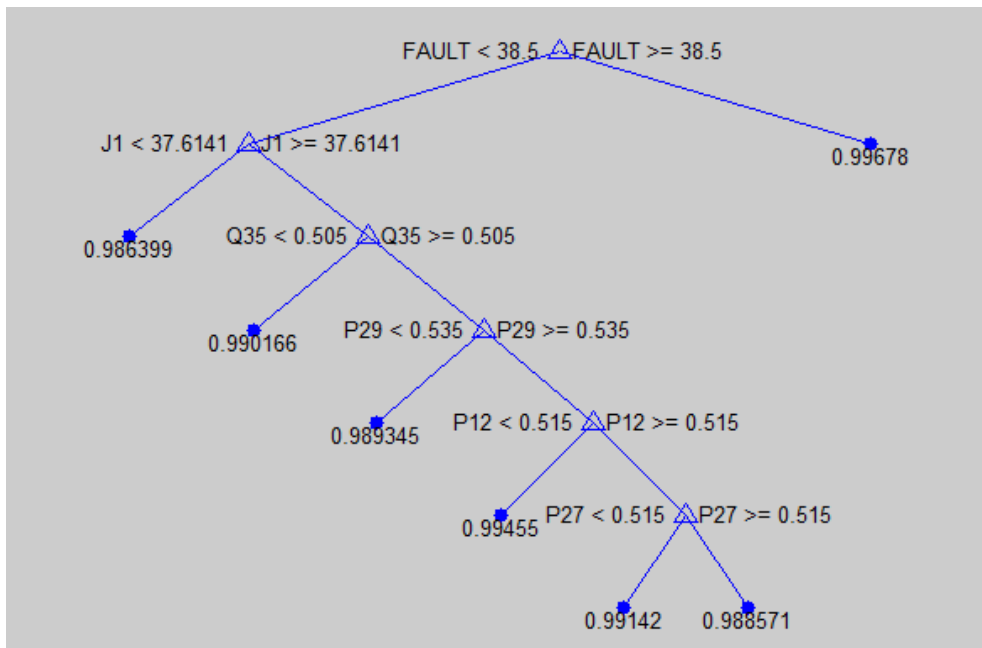


Figure A5.2: CART Tree (3500 Minimum Observations) Bus 3 – Kenya Power System

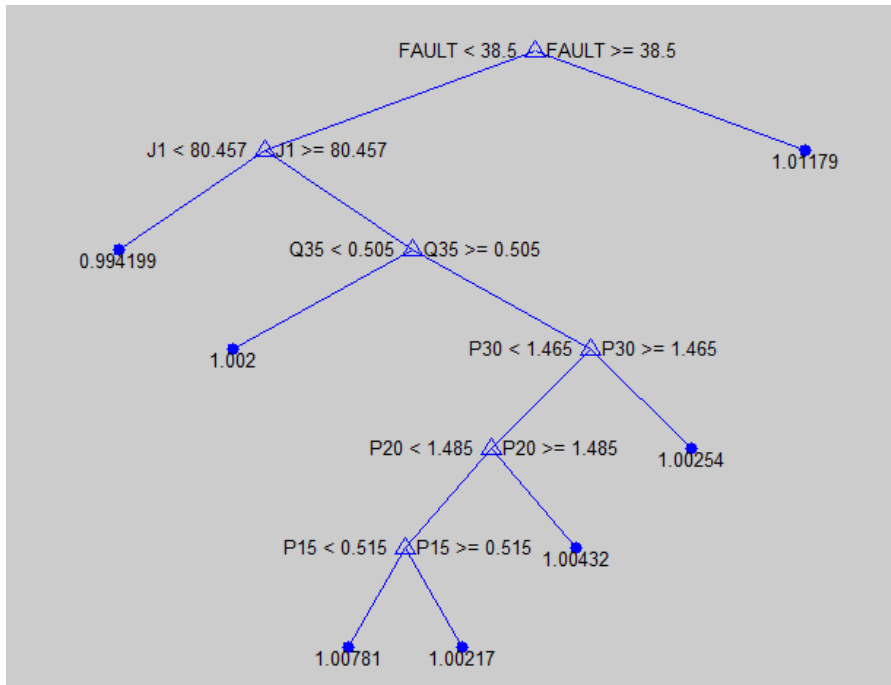


Figure A5.3: CART Tree (3500 Minimum Observations) Bus 4 – Kenya Power System

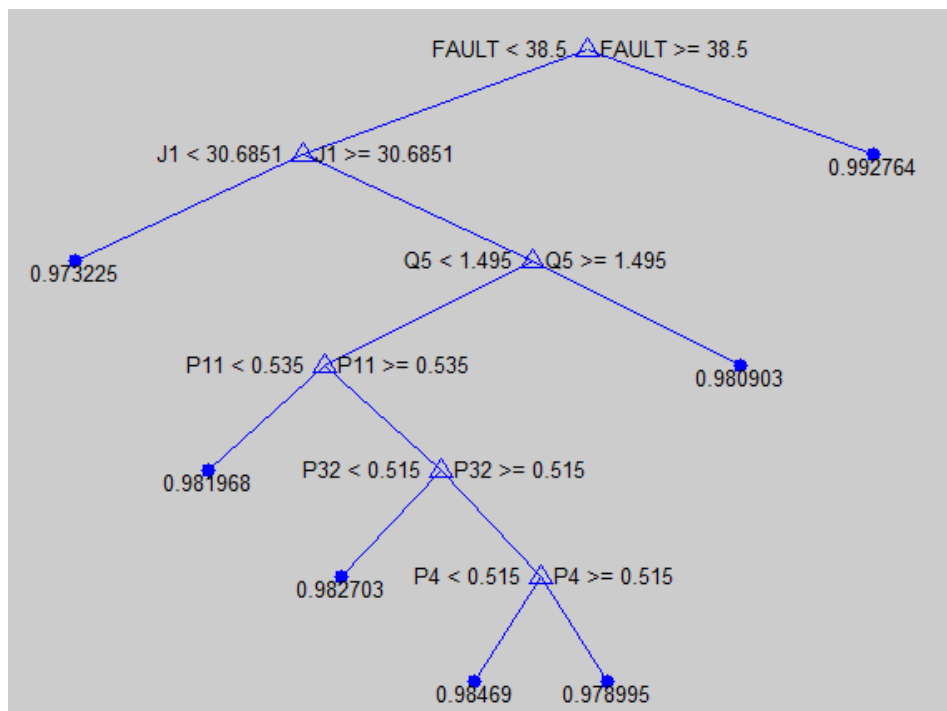


Figure A5.4: CART Tree (3500 Minimum Observations) Bus 8 – Kenya Power System

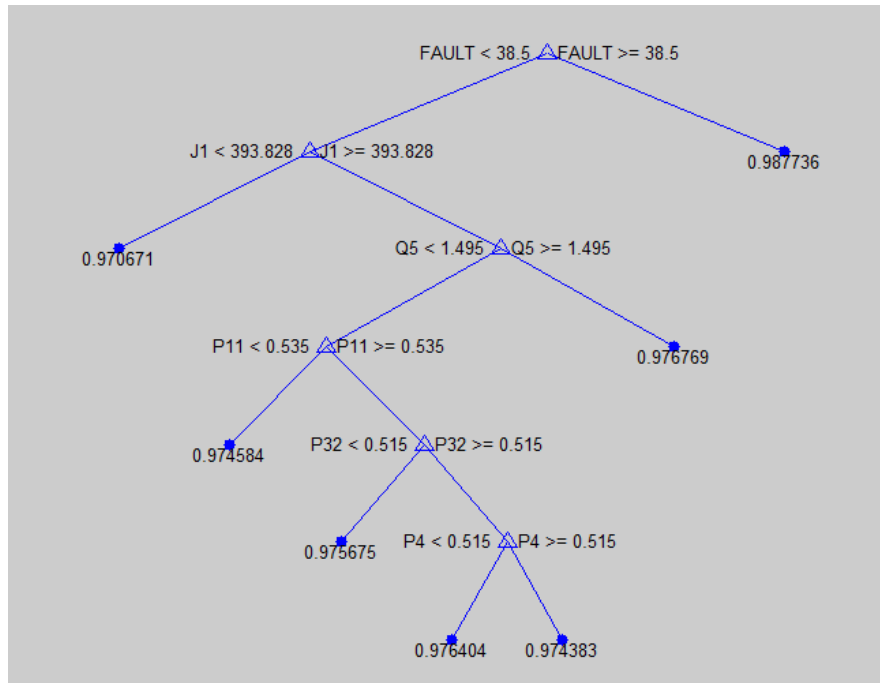


Figure A5.5: CART Tree (3500 Minimum Observations) Bus 13 – Kenya Power System

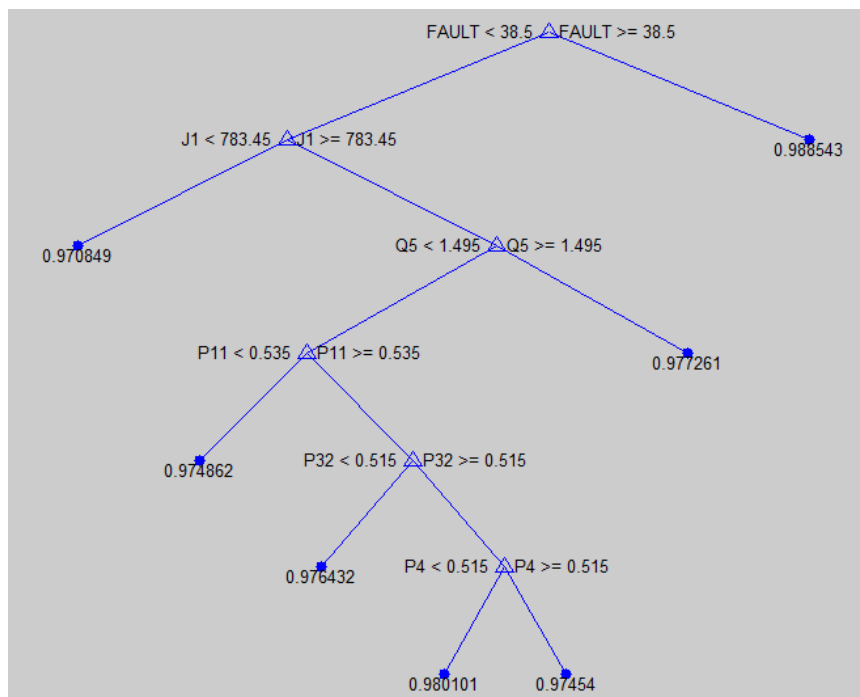


Figure A5.6: CART Tree (3500 Minimum Observations) Bus 15 – Kenya Power System

